



OPEN ACCESS

EDITED BY

Alcides Nobrega Sial,
Federal University of Pernambuco,
Brazil

REVIEWED BY

Moacir Macambira,
Federal University of Pará, Brazil
Candido Moura,
Federal University of Pará, Brazil
Lauro Cezar Montefalco De Lira Santos,
Federal University of Pernambuco,
Brazil

*CORRESPONDENCE

Fanxue Meng,
mfx1117@163.com

SPECIALTY SECTION

This article was submitted to
Geochemistry,
a section of the journal
Frontiers in Earth Science

RECEIVED 16 July 2022

ACCEPTED 20 September 2022

PUBLISHED 06 January 2023

CITATION

Meng Y, Yuan H, Wang Q, Meng F and
Ren X (2023), New geochronological
and provenance constraints on the Late
Mesozoic sedimentary formations in the
western Shandong Province and Tanlu
fault zone, China.
Front. Earth Sci. 10:995848.
doi: 10.3389/feart.2022.995848

COPYRIGHT

© 2023 Meng, Yuan, Wang, Meng and
Ren. This is an open-access article
distributed under the terms of the
[Creative Commons Attribution License
\(CC BY\)](https://creativecommons.org/licenses/by/4.0/). The use, distribution or
reproduction in other forums is
permitted, provided the original
author(s) and the copyright owner(s) are
credited and that the original
publication in this journal is cited, in
accordance with accepted academic
practice. No use, distribution or
reproduction is permitted which does
not comply with these terms.

New geochronological and provenance constraints on the Late Mesozoic sedimentary formations in the western Shandong Province and Tanlu fault zone, China

Yuanku Meng¹, Haoqi Yuan¹, Qingling Wang¹, Fanxue Meng^{1*} and Xiang Ren²

¹Research Center of Continental Dynamics, College of Earth Science and Engineering, Shandong University of Science and Technology, Qingdao, China, ²Department of Geology, Northwest University, Xi'an, China

We present new LA-ICP-MS detrital zircon U-Pb age and trace element data of the Late Mesozoic sedimentary sequences from the western Shandong and Tanlu fault zone, with the aim to constrain the depositional ages and sedimentary sources. The samples from the western Shandong have similar U-Pb age spectra, which can be divided into three major age groups, peaking age at circa 2,475–2,540 Ma, 1820–1870 Ma and 257–285 Ma, with minor Mesoproterozoic, Neoproterozoic and Paleozoic detrital zircon grains. The sample JN recovered from the Tanlu fault zone has an overwhelming majority of the Early Cretaceous detrital zircons with the age peak at circa 125 Ma, whereas the Archean and Paleoproterozoic detrital zircons are subordinate. The weighted average age of the youngest zircons show that the Santai Formation probably had begun deposition at circa 158 Ma and terminated deposition at circa 150 Ma, and the Tianjialou Formation of the Dasheng Group had begun deposition at circa 122 Ma. Our study indicates that the activity of the dinosaurs might occur during the Late Jurassic rather than the Cretaceous in the Shandong province. In addition, most detrital zircons of the studied samples are characterized by the high Th/U ratios and left-inclined REE patterns, revealing a magmatic origin. Morphologically, most detrital zircon grains characterized by angular to sub-rounded shapes indicate a middle-short distance transport from the source regions, whereas minor detrital zircon grains show rounded shapes, indicating a long-distance transport or multiphase recycling. According to detrital age populations in this study, combined with previously published data, we conclude that depositional provenances of the Santai Formation were mainly derived from the western Shandong and Jiao-Liao Belt, and minor detritus were derived from the northern part of the North China Craton and Xing-Meng orogenic belt. The sediments deposited in the Tanlu fault zone were mainly derived from the volcanic and subvolcanic rocks of the Qingshan period in the eastern Shandong, and subordinate depositional sources were from the Jiao-Liao and the basement uplift of the western

Shandong, with minor supplier being derived from the Yinshan-Yanshan orogenic belt. The detrital provenance of the Santai Formation indicates that extension of the eastern NCC occurred during the Late Jurassic. The Neoproterozoic detrital zircons play a minor role in the studied strata, indicating that the large sinistral movement of the Tanlu fault zone might have occurred at the Early-Middle Jurassic and formed a paleogeographic separation of the western Shandong and eastern Shandong (Sulu orogenic belt).

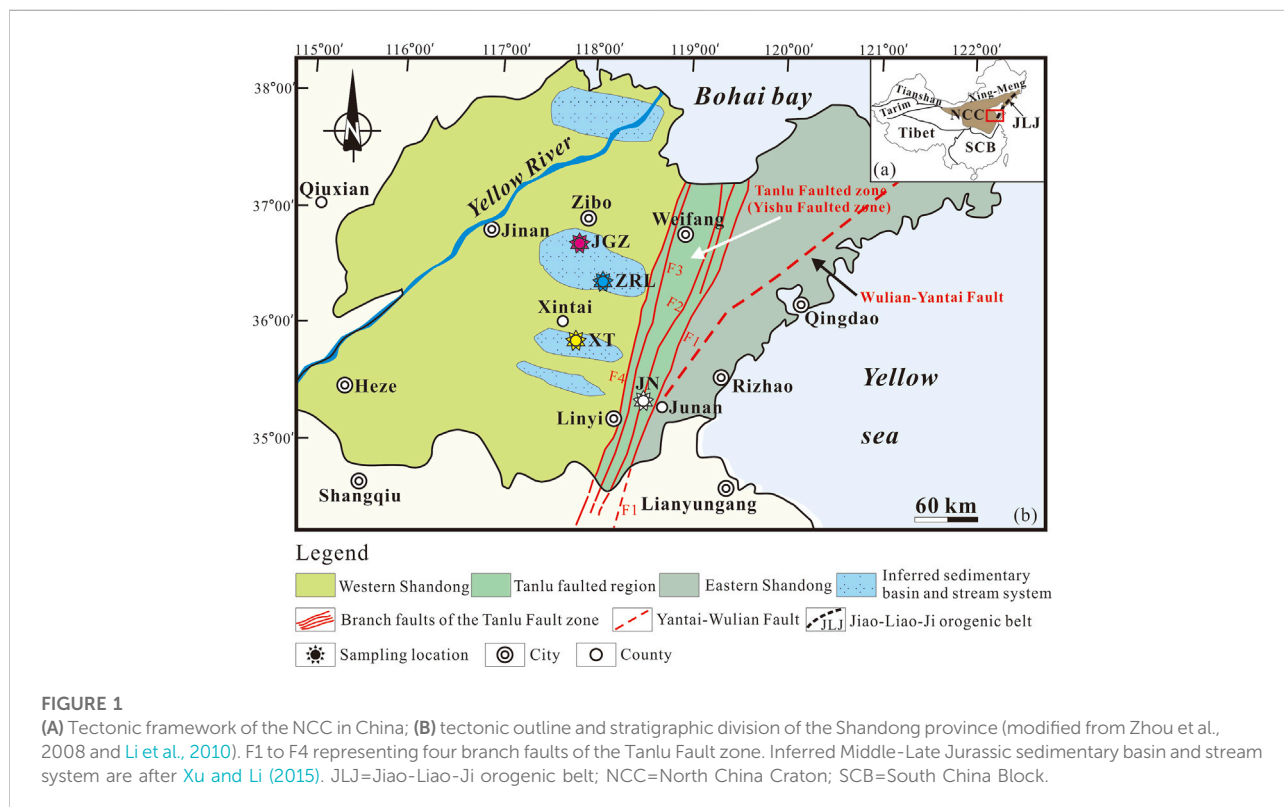
KEYWORDS

late Mesozoic, zircon U-Pb dating, depositional provenance, tectonic evolution, western Shandong province

1 Introduction

The North China Craton (NCC) (Figure 1A), one of the oldest cratons in the world, is an ideal laboratory for studying the generation and reworking of the Precambrian continental crust (e.g., Zhao et al., 2003; Xu et al., 2013; Zhai et al., 2021). During the Phanerozoic, the NCC experienced complex and significant tectono-magmatic events associated with the collision of the Yangtze terrane and subsequent Paleo-Pacific Ocean subduction, involving multiphase compressional and extensional events (e.g., Shao et al., 2000; Li et al., 2007; Yang et al., 2013; Wang et al., 2016). During the Early Cretaceous, the NCC underwent large-scale cratonic destruction and extensive lithospheric thinning from a thickness about 200 km to 60–80 km (e.g., Menzies et al., 1993; Zhang et al., 2002a;

Zhang et al., 2002b; Gao et al., 2004; Xu et al., 2004; Yang et al., 2005a; Yang et al., 2005b; Xu et al., 2008; Xu et al., 2009; Yang et al., 2009; Yang et al., 2021). Regional extensional tectonics (e.g., metamorphic core complexes and rifted and fault basins) and extensive magmatic events (I-A granitoid assemblages) have accompanied this significant cratonic destruction and lithospheric thinning in the middle Early Cretaceous (~125 Ma) (e.g., Zhu et al., 2012; Meng et al., 2020). In the whole Shandong province, the Late Mesozoic sedimentary basins/depressions are the best alternatives for studying extensional regime associated with the cratonic destruction and lithospheric thinning (Yang et al., 2013). Numerous studies have been done concerning the geochronology, petrology and geochemistry of Late Mesozoic magmatic rocks in the Shandong province (eastern NCC), and



produced large amounts of data and competing interpretations (e.g., Zhang et al., 2002a; Zhang et al., 2002b; Gao et al., 2004; Xu et al., 2004; Yang et al., 2005a; Yang et al., 2005b; Xu et al., 2008; Xu et al., 2009; Yang et al., 2009; Yang et al., 2021). By contrast, whereas little attention was paid to the well-exposed Late Mesozoic sedimentary sequences, constraining full-understanding of the NCC evolution. Therefore, systematic studies on the sedimentary rocks from the basins/depressions associated with the cratonic destruction can shed new light on the regional uplift, denudation and magmatism.

Compared to the Jiaolai basin, the sedimentary rocks distributed in the western Shandong province and the fault basins of the Tanlu fault zone are poorly constrained (Figure 1B), such as accurate depositional timing and features of source regions. Previous workers identified dinosaur and bird tracks in the studied strata (Li et al., 2005a; Li et al., 2005b; Li et al., 2015), revealing that the studied strata are essential for understanding sedimentary paleo-environment and paleo-ecology; whereas their sedimentary accurate timing is not constrained well as well. Additionally, Li et al. (2002) reported Jurassic dinosaur tracks in the Santai Formation for the first time, indicating that activity timing of dinosaurs (theropoda) might be traced to the Jurassic rather than the Cretaceous in Shandong. Due to the lack of index fossils or radiometric age data, the age of the strata of the Santai Formation is loosely constrained, involving Early-Middle Jurassic, Middle Jurassic and Late Jurassic arguments suggested by different workers (e.g., Li et al., 2002; SBGMR, 2003; Xu et al., 2013; Yang et al., 2013). Based on the above presentation, the further and systematic geochronological studies are necessary.

It has been verified that detrital zircons can provide a maximum depositional age of sediments, especially for the fossil-depauperate or Precambrian sedimentary rocks (Nelson, 2001). Compared to magmatic and metamorphic zircon, detrital zircons have a relatively complicated provenance in which they are deposited. It is well-known that detrital zircons are sourced from volcanic-sedimentary basins or convergent plate margins close to the depositional age of sediments; however, detrital zircons deposited in an extensional setting or ancient craton (lack volcanism) show older ages that reflect the history of the underlying basement far from the depositional age of the sediments (e.g., Cawood et al., 2012). The Shandong province and adjacent regions of the eastern NCC (Figure 1B), which is situated on the junction of three major tectonic domains (the Paleo-Asian Ocean, western Pacific tectonic and Tethys tectonic domains), experienced key geological events, such as the collision of the Yangtze and NCC, destruction of the NCC and Paleo-Pacific oceanic subduction as well as the closure of the Mongol-Okhotsk Ocean, resulting in extensive magmatic-volcanic events during the Mesozoic, especially the Late Mesozoic. Thus, the Shandong province, a key position of the eastern NCC, has been a hotspot for geodynamic studies.

In this study, we collected four representative samples from the Santai and Tianjialou formations (Figures 2A–D),

respectively. The Santai Formation shows a conformity contact relationship with the underlying the Fangzi Formation (Figure 3A). The Santai Formation in the Mengyin and Yiyuan regions consists mainly of brick-colored feldspar quartz sandstone and grey-white and yellow-green feldspar quartz sandstone (BGMRS, 1991). Regionally, the Santai Formation can be up to 1,000 m in thickness. Due to the lack of index fossils, the accurate depositional timing of the Santai Formation remains poorly constrained, with a broad timing range. Based on the lithology and stratigraphic contact relations, the depositional age of the Santai Formation was constrained at the Middle-Late Jurassic (SBGMR, 2003). The Tianjialou Formation deposited in the Tanlu fault zone consists of yellow-grey fine-grained sandstone, greyish shale, siltstone and silty mudstone (Figure 3B), with a thickness of 986 m along the section (BGMRS, 1991).

In this contribution, we present new LA-ICP-MS zircon U-Pb age data and trace element analyses on the sedimentary rocks from the western Shandong and Tanlu fault zone (Figure 1B and Figures 2A–D). This paper, based on the dating data of detrital zircons collected from four sandstone samples (two samples collected from sandstone occurred as dinosaur tracks), combined with regional geology and published data, aims to constrain the accurate ages of the sedimentary sequences and layers of the dinosaur tracks, and judge the source regions of the sedimentary sequences. Our new data not only provide essential data to understand sedimentary tectonic-paleogeographic configuration of the western Shandong province of the eastern NCC, but also provide critical information about the eroded orogenic belts or basements, as well as the transportation trajectories of eroded materials from the provenance. More fundamentally, our results show that the activity of the dinosaurs (theropoda) might occur in the Late Jurassic rather than the Cretaceous.

2 Regional geological background and samples

2.1 Geological background and sampling

Tectonically, the NCC is situated to the south of the Xing-Meng orogenic belt (XMOB), to the west of the Pacific plate, to the south by the Qinling-Dabie orogenic belt, to the east by the Dabie-Sulu orogenic belt (Figure 1A) (Yang et al., 2005a; Yang et al., 2005b; Li et al., 2009; Wang et al., 2020). The Shandong province, which lies in the eastern part of the NCC, has its western and eastern parts separated by the NNE trending Tanlu Fault (Figure 1B). In the Shandong region, the Tanlu fault zone, which is also called the Yishu fault zone, consists of four mainly separated branches of F1 to F4 faults (Figure 1B). The western Shandong province is situated west of the Tanlu fault zone in the southeastern part of the NCC. The eastern Shandong is located in

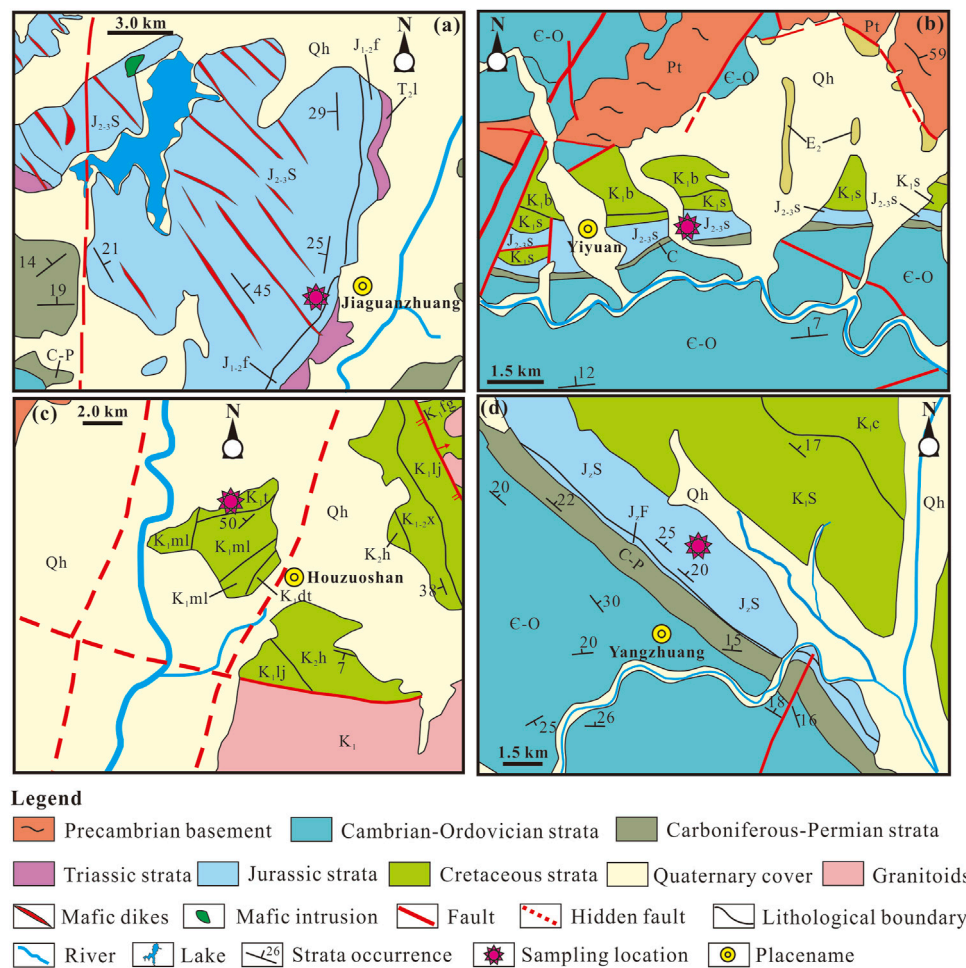
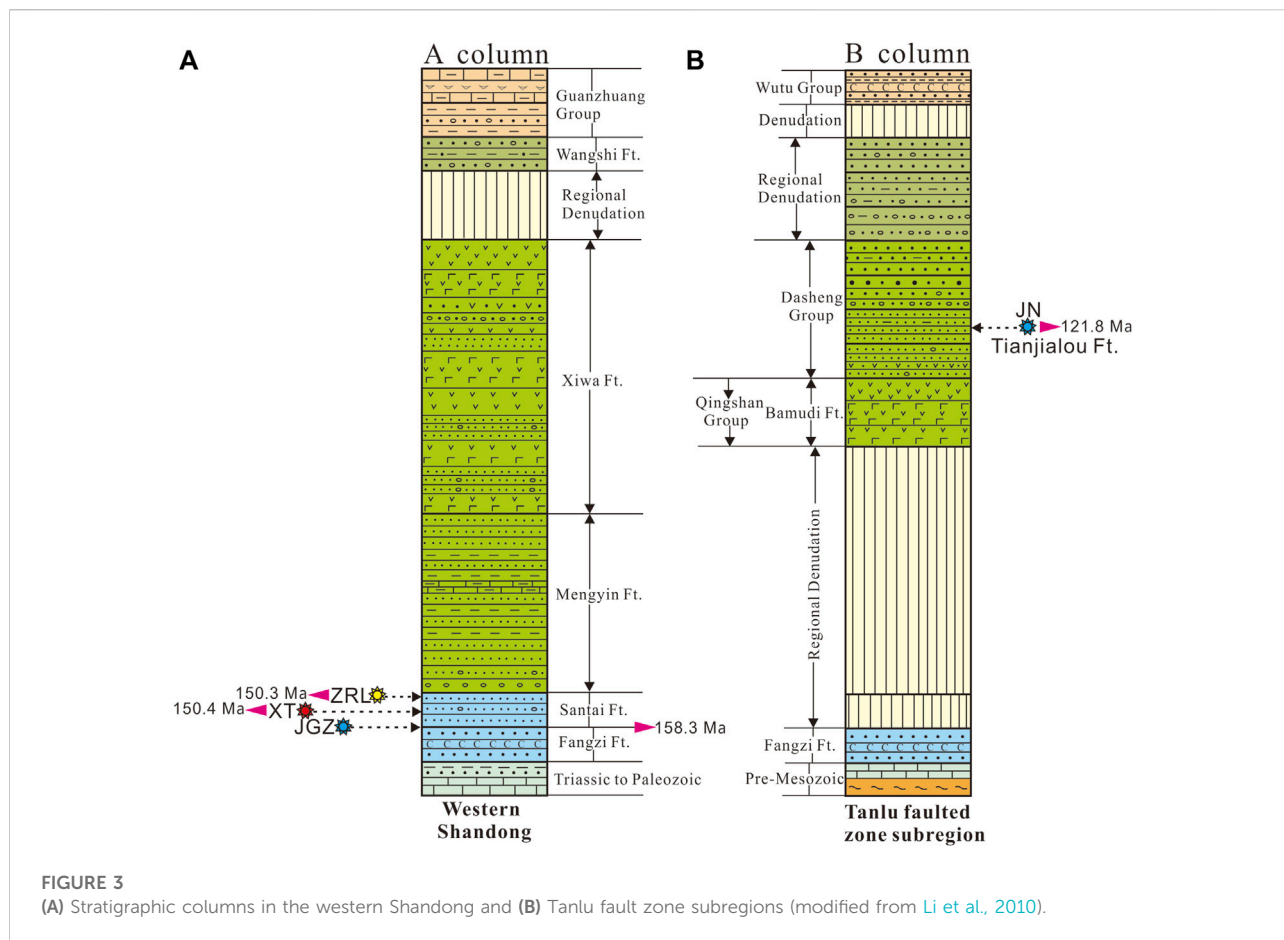


FIGURE 2

Geological and tectonic simplified map in the western Shandong and Tanlu fault zone. (A) Geological simplified map of the sample JGZ (T_2l =Liujiagou Formation; J_{1-2f} =Fangzi Formation; J_{2-3s} =Santai Formation); (B) geological simplified map of the sample ZRL (J_{2-3s} =Santai Formation; K_{1b} =Bamudi Formation; K_{1s} =Shuinan Formation); (C) geological simplified of the sample JN (K_{1fg} =Fanggezhuang Formation; K_{1t} =Tianjialou Formation; K_{1ml} =Malangou Formation; K_{1lj} =Linjiazhuang Formation; K_{1-x} =Xingezhuang Formation; K_{2h} =Hongtuya Formation) and (D) geological simplified of the sample XT (K_1c =Chengshanhou Formation; K_1s =Shuinan Formation; J_{2s} =Santai Formation; J_{2f} =Fangzi Formation).

the east of the Tanlu fault zone (Figure 1B). Similar to the tectonic divisions, the volcano-sedimentary sequences and lithostratigraphy are as well separated into three parts, the western Shandong, Tanlu fault zone and eastern Shandong (Li et al., 2010). The western Shandong province, adjacent to the Sulu orogenic belt (lied in the east of Tanlu Fault), is characterized by the Archean metamorphic rocks and the Neoproterozoic-Paleozoic unmetamorphosed sedimentary rocks, which are similar to other regions in the NCC (BGMRSD, 1991). Moreover, the western Shandong province develops the Cambrian and Early-Middle Ordovician and Carboniferous to Permian sedimentary sequences (Peng et al., 2013; Wang et al., 2013). The Late Mesozoic sedimentary sequences are mainly composed of riverine-lacustrine

sedimentary rocks in the western Shandong province (SBGMR, 2003), composed of the Fangzi, Santai, Mengyin, Xiawa, Wangshi formations and Guanzhuang Group (Gucheng and Bianqiao formations) from the bottom to the top (Figure 3A). However, the eastern Shandong province consists of Early-Late Cretaceous and Paleogene sedimentary sequences lacking Jurassic and Triassic strata, and the Late Mesozoic strata have an unconformable contact with the underlying Precambrian basement rocks. The Tanlu fault zone region consists of minor Jurassic sediments and Early-Late Cretaceous (Qingshan and Dasheng Groups) and Paleogene (Wutu Group) sedimentary sequences lacking the Early Cretaceous Laiyang Group (Figure 3B). Our study areas are



located in the western Shandong province and Tanlu fault zone (Figure 1B).

2.2 Sample descriptions

Sample JGZ was collected from the lowermost part of the Santai Formation in the vicinity of Jianguangzhuang village of Zibo city (Figure 2A), which shows extensive exposures in the field (Figures 4A,B). The field exposures show grey to greyish-green primary sedimentary colors. Additionally, the field observations show that the sample JGZ is typical fine-grained sandstone consistent with the thin section analyses, which mainly consists of quartz, feldspar and biotite and clay minerals (Figure 5A), indicating a matrix-supported texture. Microscopically, the feldspar and quartz grains are characterized by angular and sub-angular shapes, combined with detrital textures (matrix-supported) and field features, indicating a lacustrine depositional environment. In addition, the thin sections show that the feldspar grains mainly consist of K-feldspar grains characterized by typical cross-hatched twinning. The feldspar grains underwent weak chemical alteration.

The sample ZRL was collected from the Santai Formation in the Yiyuan county of the western Shandong (Figure 2B). The field observations show that the studied strata are characterized by typical oxidation colors (brick-colored) (Figures 4C,D) and cross-bedding and inclined beddings, indicating a fluvial depositional system (Figure 4D). The brick-colored sandstone shows medium-coarse grained textures, consisting of quartz, feldspar and minor mafic minerals (e.g., biotite) (Figure 5B). The quartz and feldspar grains show typical angular shapes and some feldspar grains undergo significant chemical alterations, such as sericitization and kaolinization. In addition, the thin sections show that the sample ZRL experienced a weak sorting process, reflecting a relatively low maturity. The studied sample belongs to typical grain-supported textures (Figure 5B).

The sample JN was collected from the geological park of the Houzuo mountain in Junan county of Linyin city (Figure 2C). The sample JN belongs to the Tianjialou Formation of the Dasheng Group (Figure 3B). According to previous studies (Li et al., 2005a; Li et al., 2005b), the sample JN preserved diverse dinosaur tracks and small numbers of fossil bird tracks (Figure 4E), documenting key paleo-ecological significance. The sample JN is medium- and fine-grained sandstone, and

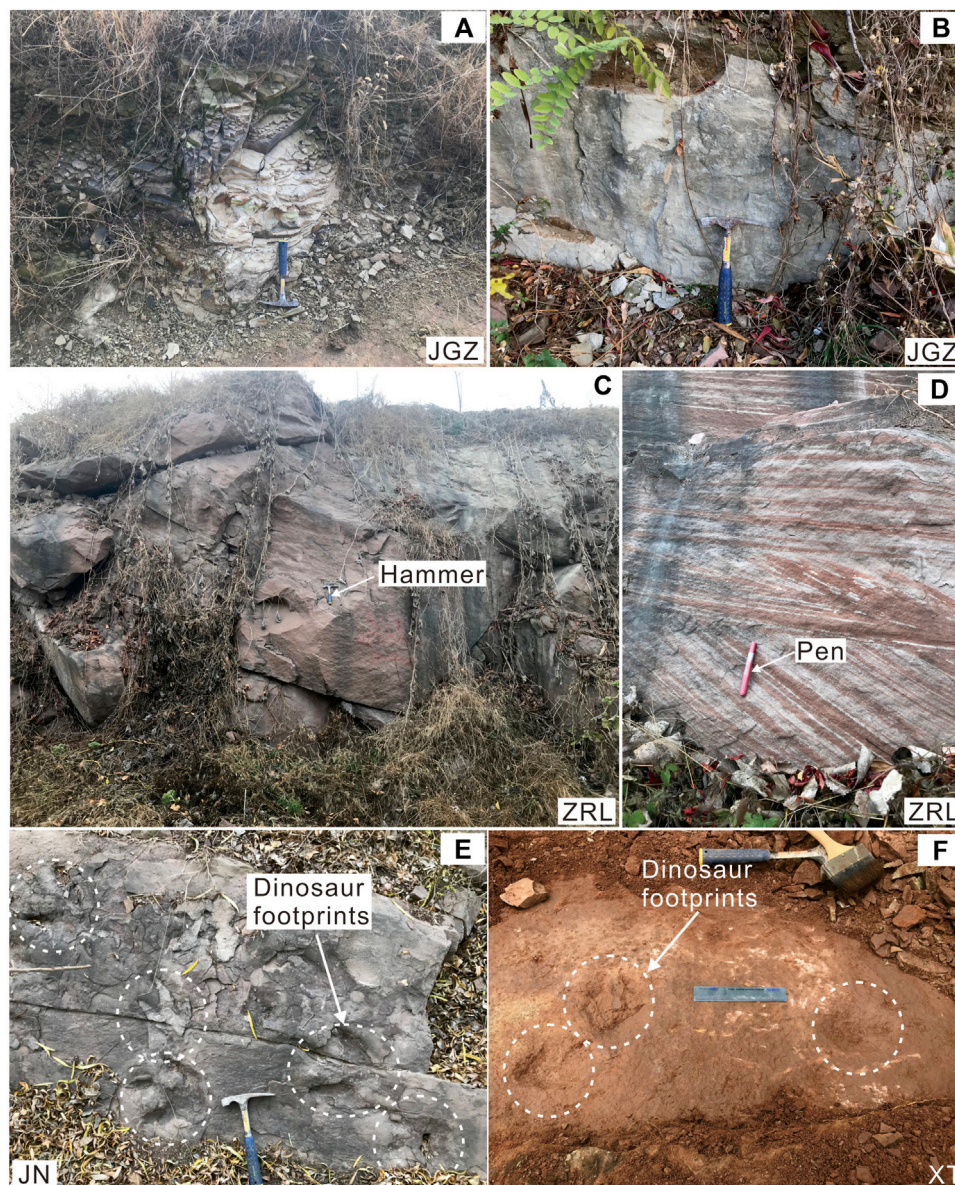


FIGURE 4

Field photographs showing outcrops and exposures of the studied samples in the western Shandong province and Tanlu fault zone. **(A–B)** Exposures of the lowermost part of the Santai Formation consisting of grey- or grey-white sandstone; **(C–D)** exposures of the upper part of the Santai Formation characterized by typical sedimentation of fluvial facies, developing typical wedge-shaped cross-bedding; **(E)** grey- or grey-white sandstone with the dinosaur tracks in the Houzuo mountain; **(F)** brick-colored sandstone with the dinosaur tracks within the upper part of the Santai Formation in the Mengyin region.

are dominated by quartz, feldspar and lithic fragments (clay matrix and volcanic fragments) with minor Fe-Ti oxides. The dominant minerals show typical angular shapes and matrix-supported textures (Figure 5E). Combined with the mineral textures, the sample JN shows relatively low compositional and textural maturity.

The sample XT was collected from the Santai Formation in the Mengyin region of the western Shandong province

(Figure 2D). Li et al. (2002) reported dinosaur (theropoda) tracks in the studied layer. The studied sample XT was undertaken from the sedimentary layer that preserves well dinosaur tracks (Figure 4F). The field observations show that the studied layer is characterized by medium- and fine-grained feldspar quartz sandstone with minor glutenite, reflecting a fluvial depositional setting. The fine-grained sandstone mainly comprises quartz and feldspar grains that show angular shapes,

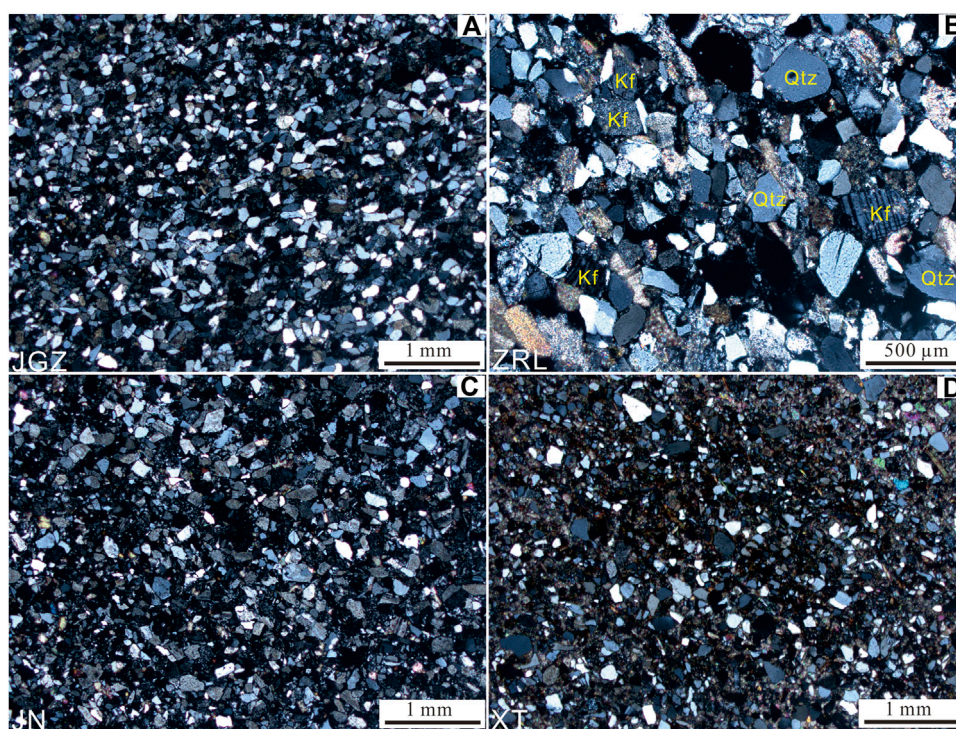


FIGURE 5

Microphotographs of the thin-sections showing the textures and mineral compositions of the four representative samples; (A) sample JGZ consisting of fine-grained quartz and feldspar with angular shapes, (B) sample ZRL consisting of intermediate-coarse grained quartz, K-feldspar and minor plagioclase grains with typical angular shapes; (C) sample JN consisting of fine-grained quartz and feldspar grains with angular shapes; (D) sample XT consisting of fine-grained felsic minerals and mafic minerals with typical matrix-supported texture.

reflecting low compositional and textural maturity (Figure 5D). Additionally, the brick-colored fine-grained sandstone contains clay minerals and fine-grained mineral fragments (Figure 5D), showing matrix-supported textures.

3 Analytical techniques

The internal structures and textures of the studied zircons were examined using cathodeluminescence (CL) imaging through a scanning electronic microprobe at the Shandong Provincial Key Laboratory of Depositional Mineralization and Sedimentary Minerals, Shandong University of Science and Technology, in order to select potential targets for U-Pb dating and trace element analyses. Four representative medium-fine and coarse-grained sandstone samples derived from the western Shandong and Tanlu fault zone were selected for LA-ICP-MS zircon U-Pb dating and trace elemental analyses (Figures 6A–D). All rocks were cleaned, and then were crushed to powders using conventional gravimetric-magnetic and liquids separation methods to separate zircons. The separated zircons were processed by hand picking under a binocular microscope. The selected zircon crystals were mounted in a 1-inch diameter epoxy that was polished to half-section for cathode-luminescence (CL) images, characterizing the internal

features of zircons. The zircon separation and CL images were performed at the Institution of Geological Survey and Mapping of Hebei Province, Langfang city, China. All analytical zircons have no cracks and inclusions.

Zircon U-Pb dating was performed at the Wuhan Sample Solution Analytical Technology Co., Ltd. (China) (WSSAT) using LA-ICP-MS (laser ablation-inductively coupled plasma-mass spectrometry) (Agilent 7700e ICP-MS instrument) following the methods of Chang et al. (2006). Helium was applied as a carrier gas. Argon was used as the make-up gas and mixed with the carrier gas via a T-connector before entering the ICP. In this study, zircon 91500 ($U=91$ ppm) (Ballard et al., 2001) and glass NIST610 were used as external standards for U-Pb dating and trace element calibration, whilst zircon ^{29}Si concentration was used for internal standardization. The recommended value is consistent with the analytical value of zircon 91,500 during the experiment, suggesting that the analytical data are reliable. The common lead correction was conducted using the ^{208}Pb method. The analytical data were processed using ICPMSDatacal9.0 software, and Concordia diagrams and weighted average ages were made using version ISOPLOT/Ex-version 4.11 embed in the Excel (Ludwig, 2003). Individual analyses in the data table and Concordia plots are present at 1σ and U-Pb age uncertainty is quoted at the 95% confidence level. The probability



FIGURE 6

Representative cathodoluminescence (CL) images of analyzed zircons from the western Shandong province and Tanlu fault zone; yellow circles showing the positions of LA-ICP-MS laser spots for age isotopic domains; samples (A, B, D) from the western Shandong province, and sample (C) from the Tanlu fault zone

density plot of detrital zircon age distribution uses the kernel density estimation (KDE) method (Vermeesch, 2012). The detailed descriptions of analytical methods were referred to Chang et al. (2006) and Zong et al. (2017). In this study, we have used the weighted average ages of the youngest zircon populations to address the maximum depositional ages of the detrital rocks.

4 Analytical results

4.1 Zircon morphology and origin

A total of 351 zircon grains from four representative samples were conducted for LA-ICP-MS U-Pb dating, among which

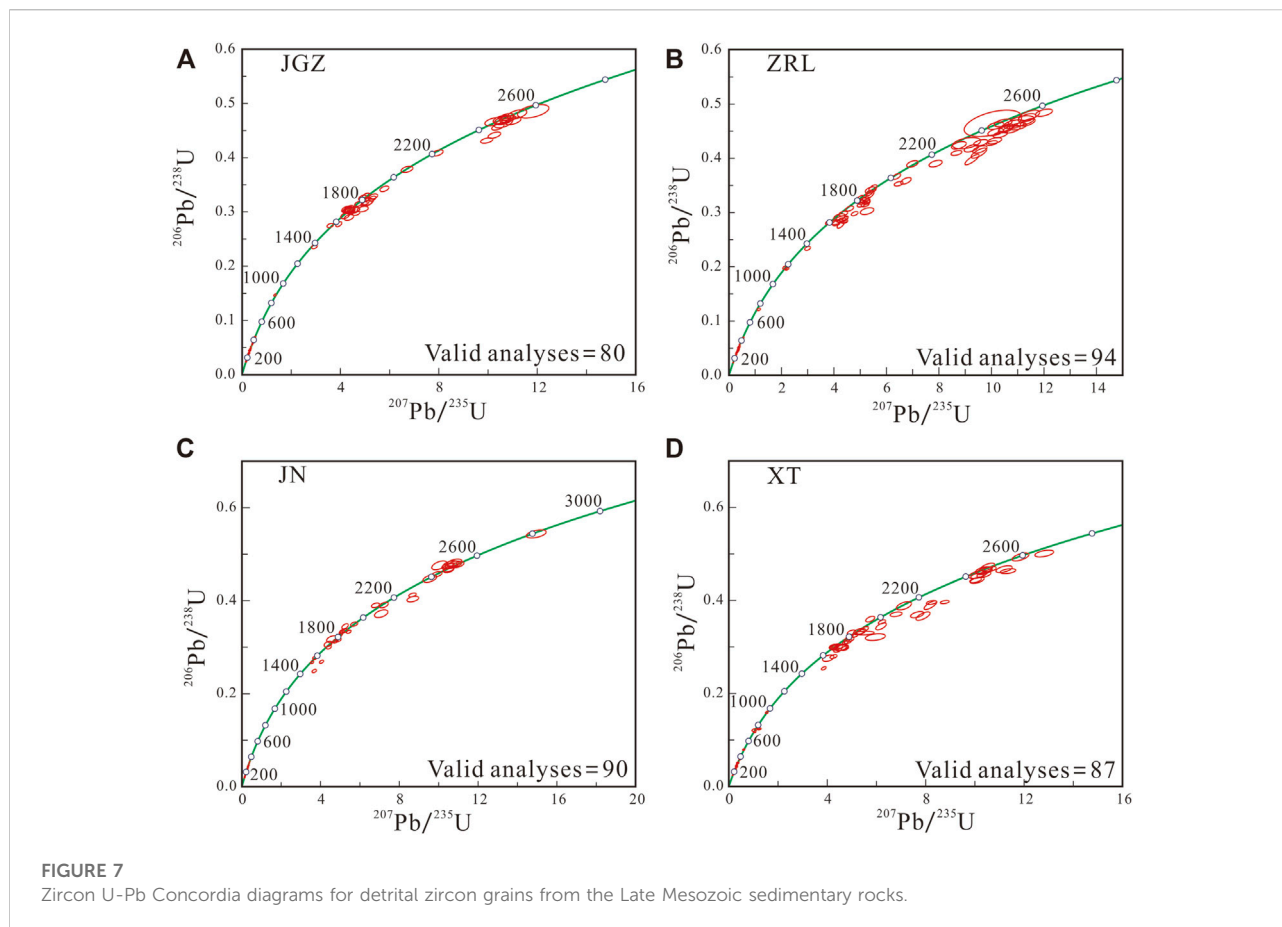


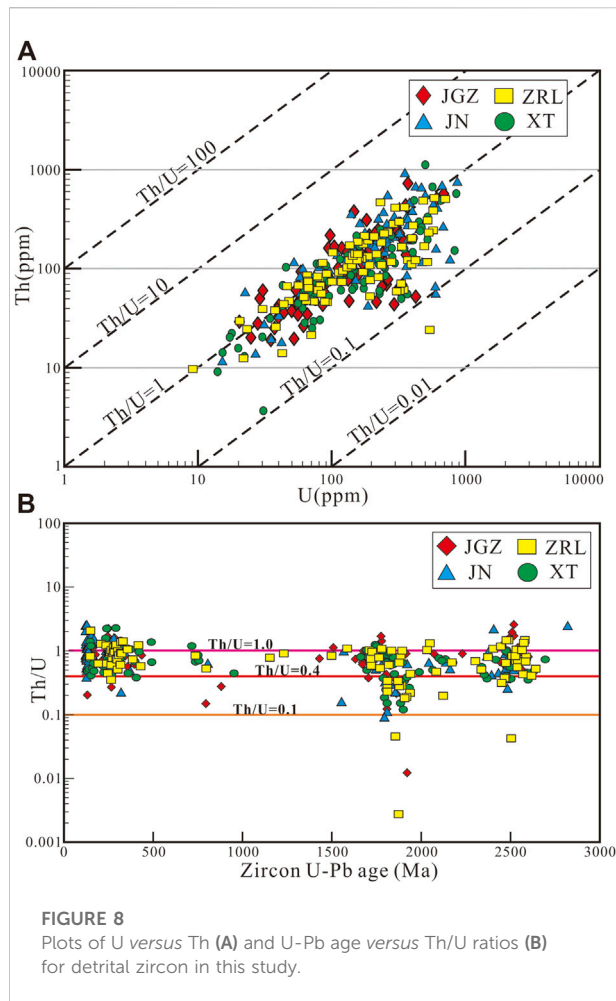
FIGURE 7

Zircon U-Pb Concordia diagrams for detrital zircon grains from the Late Mesozoic sedimentary rocks.

344 analyses (JGZ=76; JN=90; XT=84; ZRL=94) yield concordant ages (Figures 7A–D). Representative cathode luminescence (CL) images are presented in Figures 6A–D. Circa 200 zircon grains were selected for CL imaging per sample, and the studied zircon grains are colorless (light pink) to dark grey or black. These zircon grains are 40–200 μm in size, with length/width ratios of 1:1 to 5:1. The studied zircon grains have complicated CL images and morphologies exhibiting significant differences and genesis (Figures 6A–D). The CL images show that detrital zircons from four representative samples are predominantly subhedral and euhedral morphologies, with minor zircons showing rounded shapes. Moreover, most detrital zircons have oscillatory zoning textures characterized by dark grey to light-grey colors, whereas minor detrital zircons show black grey to black colors characterized by no oscillatory and spongy/skeleton or taxitic structures, reflecting a fluid-related metasomatic/metamorphic process (high U). Zircon Th/U ratios can also define zircon types. Zircon Th/U distribution patterns show that most zircons from four representative samples have high Th/U ratios (>0.4), indicative of a magmatic origin (Corfu et al., 2003; Gehrels, 2014) (Figures 8A,B).

Most of the detrital zircons from the sample JGZ show enrichment of heavy rare Earth elements (HREE) and

depletion of light rare Earth elements (LREE), reflecting a right-inclined pattern (Figure 9A). The REE patterns indicate that most detrital zircons collected from the sample JGZ have a close affinity with a magmatic origin. In addition, some detrital zircons show nearly flat HREE patterns and positive or slightly negative Eu element anomalies. The sample ZRL shows complicated REE patterns, with most analyzed detrital zircons showing depletion of the LREE and enrichment of the HREE, with minor detrital zircons showing steady LREE patterns (Figure 9B). Furthermore, most zircons have Ce positive anomalies and Eu negative anomalies (Figure 9B), consistent with a magmatic origin. The detrital zircons derived from the sample JN show that most of the detrital zircons are characterized by enrichment of HREE and depletion of LREE, with minor detrital zircons showing flat LREE patterns and weak or no significant Eu and Ce anomalies (Figure 9C). The detrital zircons from the sample XT show that most of the analyzed zircons are characterized by enrichment of HREE and depletion of LREE, with positive Ce anomalies and Eu negative anomalies, corresponding to a magmatic origin (Figure 9D). In addition, minor detrital zircons show flat REE patterns (Figure 9D). In summary, four representative samples show similar REE patterns, indicating that most analyzed detrital zircons reflect



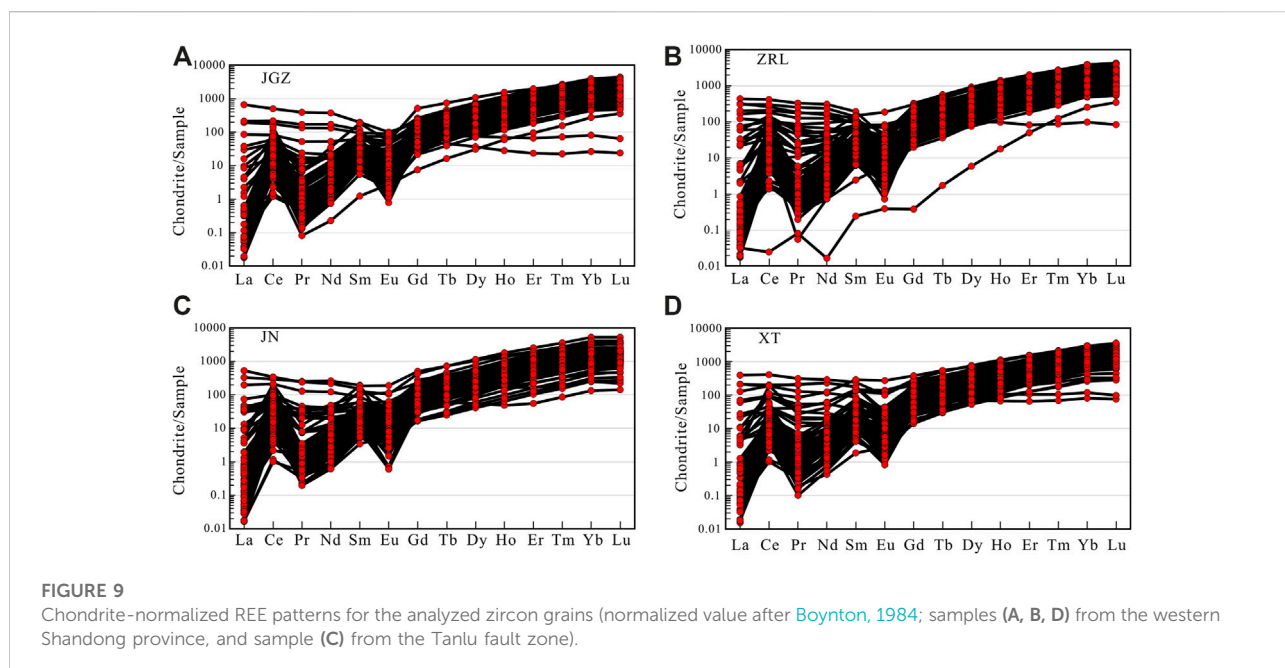
a magmatic origin characterized by enrichment of HREE and depletion of LREE, with Ce positive anomalies and Eu negative anomalies. A small number of detrital zircons show flat REE patterns and weak or insignificant Ce and Eu anomalies, not typical for magmatic zircons, indicating a complicated genesis.

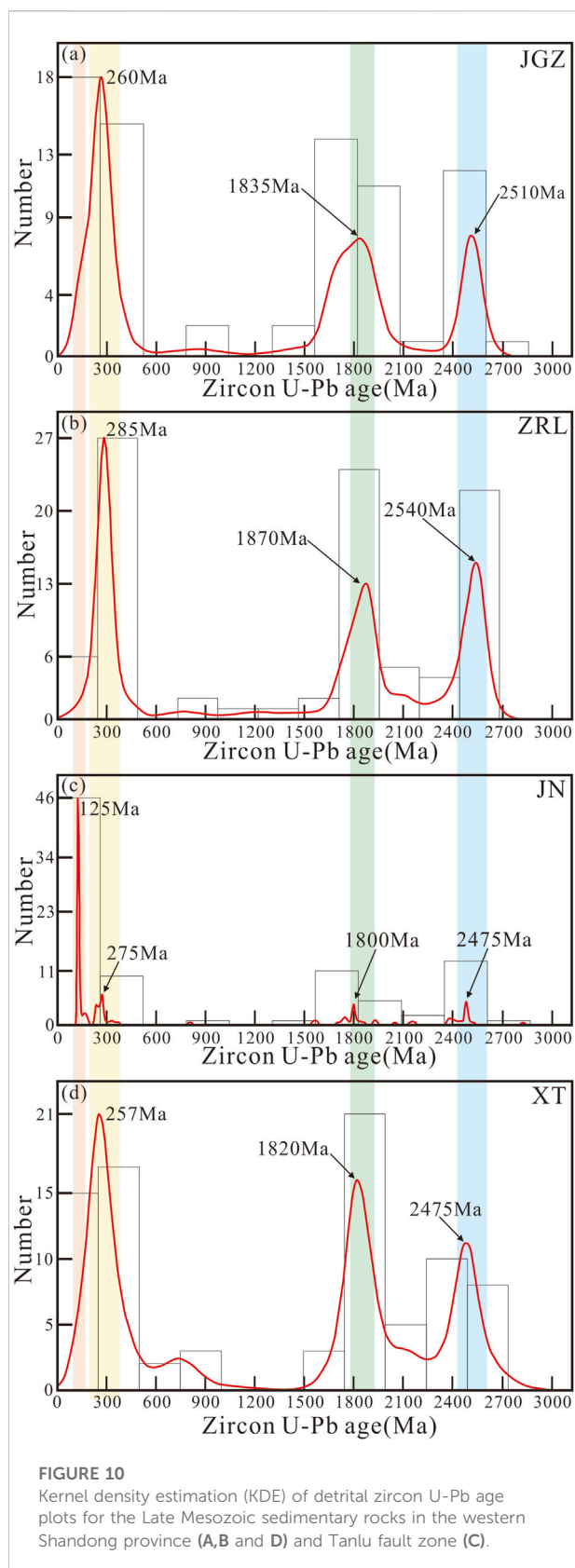
In this study, the $^{206}\text{Pb}/^{238}\text{U}$ ages were used for zircon grains less than 1.0 Ga and $^{206}\text{Pb}/^{207}\text{Pb}$ ages were used for zircon grains more than 1.0 Ga due to the imprecise measurement of ^{207}Pb in young zircons (Sircombe, 1999). The analyzed zircons with low discordance < 10% plot into the concordant curves of $^{207}\text{Pb}/^{235}\text{U}$ versus $^{206}\text{Pb}/^{238}\text{U}$ (Figures 7A–D), indicating that the detrital zircon ages are acceptable and tenable in the following discussion (no significant Pb losses). The analytical results of detrital zircons were listed in Supplementary Table S1.

4.2 Detrital zircon U-Pb ages and clusters

4.2.1 Fine-grained sandstone sample JGZ

The sample JGZ: the analyzed zircons are mostly of sub-angular to angular morphologies, with a few grains being rounded in shape (Figure 6A). The angular zircon grains indicate a near-by sedimentary provenance, whereas sub-rounded or rounded zircon grains indicate a long transport distance from their source or experience multiple recycles (Fedó et al., 2003). The CL images show that most of the analyzed zircon grains have clear oscillatory zoning. Some zircon grains show weak oscillatory and structureless textures. A few zircon grains are rounded shapes and have clear core-rim textures by new overgrowth rims (Figure 6A). The zircon ages, which are more than 10% discordance, are excluded in this study.





The sample JGZ yields a spectrum age varying from 153 ± 2.1 Ma to $2,552 \pm 35.7$ Ma (Supplementary Table S1). The major age groups are at 150–450 Ma (age peak at 260 Ma), 1,500–2070 Ma (age peak at 1835 Ma), and 2,300–2,560 Ma (age peak at 2,510 Ma), with a few Early Neoproterozoic zircons (Figure 10A). Most of the studied zircons have high Th/U ratios >0.30 , indicating an igneous origin (Hoskin and Ireland, 2000; Corfu et al., 2003). Additionally, some zircons, which are of a magmatic origin, characterized by very high Th/U ratios (up to 2.57) might be related to subsequent recrystallization. Some of them (one zircon dated at 796 Ma and two zircons dated at ca. 1922 Ma) have low Th/U ratios (<0.2) and show homogeneous zonation or structureless textures, implying a metamorphic origin or fluid-related metasomatic processes.

The sample JGZ was recovered from the lowermost part of the Santai Formation (Figure 3A), constraining well the beginning of deposition of the Santai Formation and depositional termination timing of the Fangzi Formation. The analytical results show that youngest zircon cluster range from 153 Ma to 163 Ma, with a weighted average age of 158.3 ± 3.5 Ma (MSWD=2.4; 95% confidence) (Figure 11A). All these zircons have high Th/U ratios and clear oscillatory zoning suggest an igneous origin, potentially corresponding to a magmatic event.

4.2.2 Medium-coarse brick-colored sandstone sample ZRL

The medium-coarse brick-colored sandstone sample ZRL is from the upper part of the Santai Formation (Figure 3A). The zircons separated from sample ZRL are prismatic to rounded in shape (Figure 6B). The CL images reveal that the separated zircons have complicated textures, about 40% zircons have clear magmatic oscillatory zoning, and other zircons have weak oscillatory zoning and homogeneous textures, with a few zircons having old core rimmed by new overgrowth rims. Ninety-four zircons within 10% discordance yield concordant ages ranging from 149 ± 3.0 Ma to $2,545 \pm 19.3$ Ma (Supplementary Table S1), and can be divided into three dominant age populations at 240–430 Ma (age peak=285 Ma), 1700–1950 Ma (age peak=1870 Ma) and 2,410–2,550 Ma (age peak=2,540 Ma), with minor age clusters at 149–210 Ma and 1975–2,400 Ma (Figure 10B). The Mesozoic zircon grains (149–247 Ma) have oscillatory zoning and high Th/U ratios of 0.44–2.03, indicating a magmatic origin. The youngest two zircon grains, characterized by high Th/U ratios of 0.80 and 2.03, have $^{206}\text{Pb}/^{238}\text{U}$ ages of 149–151 Ma, with a weighted average age of 150.3 ± 3.4 Ma (MSWD=0.16) (Figure 11B).

4.2.3 Fine-grained sandstone sample JN

Zircon grains collected from the sample JN are prismatic to rounded in shape (Figure 6C). The CL

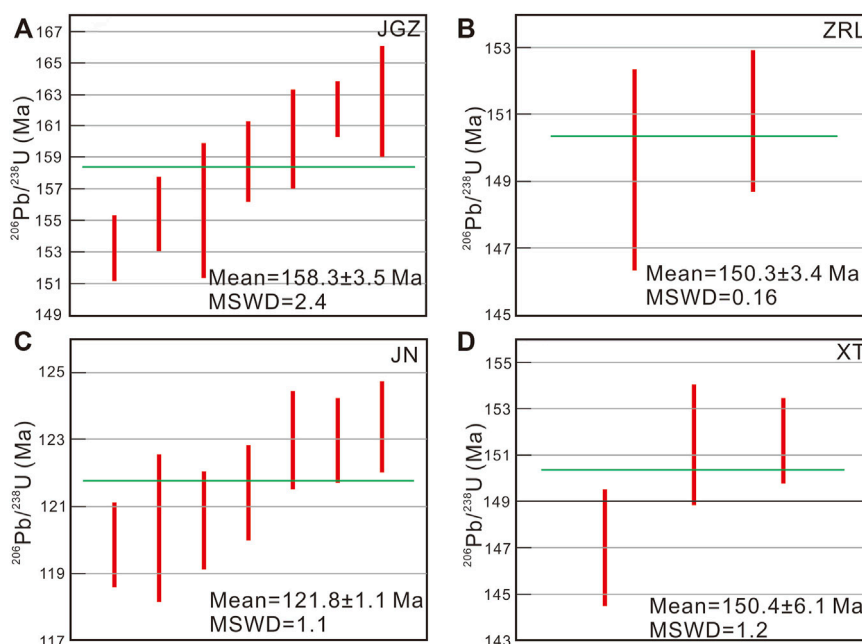


FIGURE 11

Weighted average ages of the youngest detrital zircons from the Late Mesozoic sedimentary rocks in the western Shandong province (A,B and D) and Tanlu fault zone (C).

images show that most of the zircons demonstrate oscillatory zoning, but some zircon grains are sub-rounded to rounded shapes characterized by weakly zoned and homogenous textures. The ninety zircon U-Pb analyses within 10% discordances and yield a wide spectrum age ranging from 120 ± 1.3 Ma to $2,821 \pm 37.6$ Ma (Supplementary Table S1). They yield one major age cluster at 120–250 Ma (peak at 125 Ma), with several minor clusters at 250–370 Ma (peak at 275 Ma), 1,550–1920 Ma (peak at 1800 Ma) and 2,340–2,520 Ma (peak at 2,475 Ma) (Figure 10C). Compared to other three samples, more Early Cretaceous zircons were found in this sample (Figure 10C). The youngest age clusters (120–250 Ma) have oscillatory zoning and high Th/U ratios of 0.39–2.57, indicating that they were originated from a magmatic origin. Combined with the CL images, the zircons from the youngest age cluster are mainly prismatic shapes, corresponding to an adjacent volcano-magmatic event. Some Early Mesoproterozoic and Late Paleoproterozoic zircon grains show black gray colors characterized by homogeneous zonation or structureless textures with relatively low Th/U ratios of 0.09–0.16. The youngest $^{206}\text{Pb}/^{238}\text{U}$ age cluster range from 120 to 123 Ma, with a weighted average age of 121.8 ± 1.1 Ma (MSWD=1.1; 95% confidence) (Figure 11C). These youngest zircon grains have Th/U ratios of 0.78–2.52, indicating a magmatic origin as well (Corfu et al., 2003).

4.2.4 Argillaceous sandstone sample XT

Similar to the sample ZRL, the sample XT collected from the upper part of the Santai Formation in the Mengyin basin of the western Shandong province (Figure 3A), ca. 300 m northwest of Yangzhuang village. Eighty-four zircon analyses within 10% discordance, yield concordant ages of 147–2,694 Ma (Supplementary Table S1), which fall into three major age populations, 140–420 Ma (age peak=257 Ma), 1740–1900 Ma (age peak=1820 Ma), 2,300–2,700 Ma (2,475 Ma) (Figure 10D). Minor Early Neoproterozoic zircons were also found. All analyzed zircons have relatively high Th/U ratios of 0.12–2.27. The youngest age populations (147–291 Ma) with high Th/U ratios of 0.41–2.27, combined zircon angular shapes, indicate a magmatic origin and near-by provenance (Corfu et al., 2003). Three youngest zircon grains have $^{206}\text{Pb}/^{238}\text{U}$ ages of 147–152 Ma, with a weighted average age of 150.4 ± 6.1 Ma (MSWD=1.2) (Figure 11D). Three youngest zircon grains also have high Th/U ratios of 0.41–1.4, showing the features of magmatic origin.

5 Discussion

5.1 Depositional timing of the Santai and Tianjialou formations

Generally, the youngest zircon grains can provide useful information about maximum depositional age of sediments

(Andersen, 2005; Dickinson and Gehrels, 2009; Cawood et al., 2012). However, multiple studies have shown that the youngest detrital zircon grains might do not provide the most accurate estimates of depositional age (Andersen, 2005). The youngest zircon cluster can greatly predate deposition due to Pb loss of detrital zircons (Gehrels, 2014). The weighted average age of the detrital zircons can reduce these types of uncertainty (Dickinson and Gehrels, 2009). Therefore, we use the weighted average age of the detrital zircons to constrain maximum depositional age in this study.

The Santai Formation is widely distributed in the western Shandong province, conformably underlying the Fangzi Formation. As discussed above, the depositional age of the Santai Formation is poorly constrained due to the lack of the index fossils (Li et al., 2002; Yang et al., 2013). In this study, we collected one sample from the lowermost part of the Santai Formation (sample JGZ). Among the youngest grains, seven zircon grains from the sample JGZ yield $^{206}\text{Pb}/^{238}\text{U}$ ages of 153–163 Ma, with a weighted average age of 158.3 ± 3.5 Ma (MSWD=2.4) (Figure 11A). The data indicate that the Santai Formation began sedimentation at circa 158.3 ± 3.5 Ma (Figure 11A), indicating depositional termination of the Fangzi Formation.

The samples ZRL and XT both were collected from the upper part of the Santai Formation in Yiyuan and Mengyin areas of the western Shandong province, yielding 150.3 ± 3.4 Ma and 150.4 ± 6.1 Ma (Figures 11B,D). Therefore, we regard ca. 150 Ma as the depositional termination of the Santai Formation in the western Shandong province. Furthermore, the accurate dating results also suggest that dinosaurs (theropoda) began seeking activities in the western Shandong province during the Late Jurassic rather than the Cretaceous.

The youngest zircon grains from the sample JN yield a weighted average age of 121.8 ± 1.1 Ma (Figure 11C), which is regarded as the best estimate for the maximum age of deposition of the Tianjialou Formation. According to Palaeoecology features within the Tianjialou Formation, Li et al. (2005a, b) argued that the dinosaur and bird tracks were formed in the Barremian to Aptian stages of the Early Cretaceous. Our result further indicates that the depositional layer that developed dinosaur and bird tracks were formed at circa 122 Ma.

In summary, our combined results suggest that the Santai Formation probably began deposition at the early Late Jurassic (158.3 Ma-Oxfordian stage) and terminated deposition at the Late Jurassic (150 Ma-Tithonian stage). The Tianjialong Formation of the Dasheng Group was deposited after the Barremian stage of the Early Cretaceous (~122 Ma).

5.2 Analysis of potential depositional sources

As shown in Figure 10, all detrital U-Pb data indicate four major age populations in this study, including the Late

Neoproterozoic to Earliest Paleoproterozoic, Late Paleoproterozoic, Early-Middle Permian and Early Cretaceous. In this section, we will discuss the potential depositional provenance of each age population of each sample separately.

5.2.1 Neoproterozoic to Paleoproterozoic detrital zircons

Zircon U-Pb dating results show that four representative samples have Archean to Paleoproterozoic age populations (Figures 10A–D). The sample JGZ have thirty-nine Neoproterozoic to Paleoproterozoic detrital zircons ranging from 1,633 Ma to 2,601 Ma, and most detrital zircons have Th/U ratios of 0.20–2.57, indicating that they were originated from a magmatic origin. Only two detrital zircons dated at 1922 Ma and 1809 Ma have the low Th/U ratio of 0.01 and 0.12, which shows rounded shape and have no obvious oscillatory zoning textures, reflecting multiple recycles or a long-distance transportation. The age populations concentrate on Latest Neoproterozoic (circa 2,500 Ma) and Middle-Late Paleoproterozoic (peak at circa 1835 Ma) (Figure 10A). The sample JGZ contains thirteen detrital zircons ranging from 2443 Ma to 2,601 Ma, with high Th/U ratios of 0.5–2.57, corresponding to a magmatic origin. Most of zircons show sub-rounded to angular shapes and weak oscillatory zoning, with two zircons having rounded shapes, indicating a near-by deposition. The sample ZRL contains fifty-five Neoproterozoic to Paleoproterozoic detrital zircons ranging from 1713 Ma to 2,644 Ma. Most of zircons have wide ranges of Th/U ratios of 0.18–1.45, with most zircons having Th/U ratios, reflecting a magmatic origin (Corfu et al., 2003). Three detrital zircons have low Th/U ratios <0.1, which contain two zircon grains dated at 1857 and 1876 Ma with sub-rounded to angular shapes, and one zircon grain dated at 2,506 Ma with angular shapes. These three zircons show weak or no obvious oscillatory zoning, with one zircon dated at 2,506 Ma showing clear core-rim texture and other two zircons showing dark-grey colors. The sample JN has two Neoproterozoic detrital zircons dated at 2,818 Ma and 2,518 Ma, with high Th/U ratios and sub-rounded morphologies, suggesting a magmatic origin (Corfu et al., 2003). The results show that the sample JN has twenty-nine Paleoproterozoic detrital zircons ranging from 1,698 Ma to 2,492 Ma (age peak=1800 Ma and age peak=2,475 Ma) (Figure 10C). These Paleoproterozoic zircons show complicated textures, and most of the detrital zircons show sub-rounded shapes with weak or no oscillatory zoning textures. Few zircon grains show rounded shapes and no oscillatory zoning textures, and one detrital zircon dated at 2,484 Ma has dark grey color and low Th/U ratio of 0.26, suggesting a metasomatic/metamorphic effect (Rubatto, 2017). The sample XT has forty-seven Neoproterozoic to Paleoproterozoic detrital zircons that have $^{207}\text{Pb}/^{206}\text{Pb}$ ages of 1,661 Ma to 2,694 Ma, most zircons with Th/U ratios 0.12 to 1.25, reflecting a magmatic origin (Corfu et al., 2003). Most of the Archean to Paleoproterozoic detrital zircons have sub-rounded

to angular shapes, with weak oscillatory zoning. Few grains have rounded shapes that might be related to multiple recycles or a long transportation. Among the Neoproterozoic to Paleoproterozoic detrital zircons, there are two significant age populations of Earliest Statherian stage of the Paleoproterozoic (circa 1800 Ma) and Latest Neoproterozoic (circa 2,500 Ma) (Figure 10D).

The eastern NCC comprises northern NCC, the Liaodong Peninsula and the Jiaobei terranes. It is well-constructed that the eastern NCC is characterized by the Neoproterozoic and Paleoproterozoic basement, but the Sulu orogenic belt is characterized by the middle Neoproterozoic magmatism and Triassic UHP metamorphic events, reflecting a close affinity with the Yangtze terrane (e.g., Hacker et al., 1998; Zheng et al., 2006; Meng et al., 2018; Meng et al., 2020). Compared to the northern NCC, the western Shandong province has two dominant peak ages between 2.75–2.7 Ga and 2.6–2.56 Ga besides the 2.5 Ga peak age (e.g., Jahn et al., 2008; Ren et al., 2016). In contrast, the Jiaobei terrane is characterized by ~2.7 Ga and 2.9 Ga (e.g., Jahn et al., 2008; Liu et al., 2013). The basement of the western Shandong province can be divided into three belts, belt A consisting of Late Neoproterozoic granitoid rocks and migmatite, belt B consisting of Early Neoproterozoic granitoid rocks and supracrustal rocks, and belt C mainly consisting of Late Neoproterozoic mafic rocks (Wan et al., 2010; Wan et al., 2011). Compared to the western Shandong province, the Paleoproterozoic rocks mainly comprise the Jingshan and Fenzishan Groups, and the Late Neoproterozoic and Late Paleoproterozoic magmatic events were extensive in the Jiaodong region (Jahn et al., 2008; Zhou et al., 2008; Tam et al., 2011; Wu et al., 2014; Xie et al., 2014; Wan et al., 2020).

In this study, the samples (JGZ, ZRL and XT) were recovered from the western Shandong province, recording two dominant age peaks of ca. 2,500 Ma and ca. 1850 Ma (Figures 10A,B,D). As shown above, the Late Neoproterozoic to Early Paleoproterozoic magmatic activities and Middle-Late Paleoproterozoic magmatic events were widespread in the whole western Shandong province and Jiaodong regions of the NCC (e.g., Wan et al., 2010; Wan et al., 2011; Ren et al., 2016; Wan et al., 2020; Zhai et al., 2021). In the western Shandong province, the age of ca. 2,500 Ma is predominantly recorded by granitoids, TTG gneiss and coeval mafic volcanic rocks (e.g., Jahn et al., 1988; Wan et al., 2012). Therefore, based on age populations of the detrital zircons, we argue that the uplift of the western Shandong province is the predominant depositional source region for the samples collected from the western Shandong province (west of the Tanlu fault). The Early (2.2–2.0 Ga) and Late (2.0–1.8 Ga) Paleoproterozoic magmatic-metamorphic events were extensive in the Jiao-Liao Belt (Luo et al., 2008; Liu and Liu, 2015; Wang et al., 2017; Xie et al., 2022). Based on the CL images of the Paleoproterozoic detrital zircons and patterns of the zircon trace elements, we argue that the Jiao-Liao Belt might be the dominant supplier for the 2.2–2.0 Ga and 2.0–1.8 Ga detrital zircons. In summary, we argue, therefore, that the circa 2.5 Ga and circa 1800 Ma detrital

zircons might be derived from the uplift of the western Shandong and Jiao-Liao Belt. In contrast, the 1800 Ma and 2,475 Ma age clusters are subordinate components for the sample JN, indicating that the Jiao-Liao Belt and the basement uplift of the western Shandong province were not the dominant source area for the sedimentary deposits of the Tanlu Fault zone.

5.2.2 Mesoproterozoic detrital zircon

Mesoproterozoic detrital zircons have a minor component in this study (Figures 10A–D). The sample JGZ contains two detrital zircon grains dated at 1,431 Ma and 1,509 Ma. These two detrital zircons have high Th/U ratios of 0.76 and 1.12, and show sub-rounded shapes, corresponding to a long-distance transport or multiphase recycling. The sample ZRL contains four Mesoproterozoic detrital zircons, dated at 1,155 Ma, 1,233 Ma, 1,500 Ma and 1,588 Ma. The 1,500 Ma and 1,588 Ma detrital zircons show rounded shapes, corresponding to a long-distance transport or multiphase recycling, and 1,155 Ma and 1,233 Ma detrital zircons have sub-rounded to angular shapes. Additionally, these zircons have high Th/U ratios of 0.77–1.07, corresponding to a magmatic origin (Corfu et al., 2003). The samples JN and XT have no finding of the Mesoproterozoic detrital zircons, indicating no input of the Mesoproterozoic detritus.

The NCC have developed three Mesoproterozoic magmatic-related rifted belts (e.g., Zhai, 2004; Liu and Liu, 2015), such as the Xiong'er, Yanliao and Zhaertai-Bayan obo-Huade rifted belts. The Jixian System of the Yanliao rifted belt occurs at 1,437 Ma, 1,485 Ma and 1,560 Ma volcanic tuff; the volcanic clastic rocks of the Bilute Formation of the Huade rifted belt were formed at circa 1,515 Ma. Combined with the zircon CL shapes and textures, we argue that 1,431 Ma detrital zircon might be derived from the Tieling Formation (tuff) of the Jixian System. The 1,588 Ma detrital zircon might have been derived from the Gaoyuzhuang Formation of the Jixian System of the Yanliao rifted belt, and 1,500 Ma and 1,509 Ma detrital zircons might be derived from the Bilute Formation of the Huade rifted belt (Huade Group).

5.2.3 Neoproterozoic detrital zircon

Similar to the Mesoproterozoic detrital zircons, the Neoproterozoic detrital zircons are as well minor components in the studied units (Figures 10A–D). The sample JGZ contains two Neoproterozoic detrital zircons (dated at 796 Ma and 882 Ma), which show Th/U ratios of 0.15 and 0.28. The 796 Ma detrital zircon show rounded shape and weak oscillatory growth zoning, probably indicating multiphase recycling. The detrital zircon dated at 882 Ma shows clear oscillatory zoning and angular shape, corresponding a near-by deposition. The sample ZRL contains two Neoproterozoic detrital zircons (dated at 739 Ma and 798 Ma), which have high Th/U ratios of 0.52 and 0.83 and sub-rounded to angular shapes, indicating a magmatic origin and near-by deposition. The sample JN contains one Neoproterozoic zircon dated at

805 Ma. This zircon shows weak oscillatory zoning and angular shape, with high Th/U ratio of 0.64, indicating a magmatic origin and near-by deposition. The sample XT contains five Neoproterozoic detrital zircons ranging from 716 Ma to 952 Ma. These zircons are greyish and sub-rounded to angular shapes, with Th/U ratios of 0.44–1.19, revealing a magmatic origin and near-by deposition.

It is well-known that the Yangtze terrane is characterized by widespread Neoproterozoic magmatic events from 900 Ma to 700 Ma (mostly younger than 890 Ma) (e.g., Hacker et al., 1998; Zheng et al., 2006; Zheng et al., 2008; Meng et al., 2018; Meng et al., 2020). Although minor Neoproterozoic magmatism was reported in the southern part of the NCC, which mainly was older than 890 Ma (e.g., Peng et al., 2011a; Peng et al., 2011b; Wang et al., 2012; Yang et al., 2012). Therefore, the Neoproterozoic zircon ages still discriminates the Yangtze terrane from the NCC (e.g., Tang et al., 2008). In this study, the Neoproterozoic zircon ages are younger than 890 Ma from the western Shandong and the Tanlu fault zone, which might have been derived from the Yangtze terrane rather than the southern part of the NCC. The Sulu orogenic belt has a close affinity with the Yangtze terrane, thus the Sulu belt is characterized by the predominance of the Neoproterozoic zircon ages and minor Triassic magmatic and metamorphic ages. The protolith ages of the magmatic and metamorphic rocks are consistent with the Neoproterozoic ages in the Sulu belt (e.g., Zheng et al., 2006; Tang et al., 2008; Liu and Liou, 2011; Meng et al., 2018; Meng et al., 2020). Furthermore, the Neoproterozoic zircons show sub-rounded and angular shapes and lack overgrowths, indicating a near-by deposition. Based on the above discussion, we argue the Neoproterozoic detrital zircons were derived from the Neoproterozoic protoliths of the Sulu orogenic belt. This also indicates that the protoliths of the Sulu belt have been exhumed to the surface during the Late Jurassic. Interestingly, the Sulu orogenic belt is nearby the studied regions, but the Neoproterozoic detrital zircons are minor, indicating that the Tanlu fault zone had been a natural barrier that prohibited the detritus from the Sulu belt.

5.2.4 Paleozoic detrital zircons

The sample JGZ contains seventeen Paleozoic detrital zircons ranging from 255 Ma to 437 Ma, with high Th/U ratios of 0.27–2.23. Except a 437 Ma detrital zircon, the remnant detrital zircons belong to the Late Paleozoic. The detrital zircon dated at 437 Ma has a high Th/U ratio of 0.85 and weak oscillatory zoning, indicating a magmatic origin. The other zircons range from 255 Ma to 396 Ma characterized by sub-rounded to angular shapes, with Th/U ratios of 0.27–1.59. The sample ZRL contains twenty-six Paleozoic detrital zircons ranging from 252 Ma to 431 Ma, which can be divided into two groups, Early Paleozoic and Late Paleozoic. Two Early Paleozoic detrital zircons dated at 419 Ma and 431 Ma have high Th/U ratios of 0.57 and 1.21, indicating a magmatic origin. They have

angular shapes and clear oscillatory zoning textures. Besides the Early Paleozoic detrital zircons, the Late Paleozoic detrital zircons are predominant and mainly show angular shapes and oscillatory zoning, with high Th/U ratios of 0.34–1.39, reflecting a near-by sedimentation and magmatic origin. The sample JN contains twelve detrital zircons ranging from 255 Ma to 370 Ma, belonging to the Late Paleozoic. These zircons show sub-rounded to angular shapes and oscillatory zoning textures characterized by high Th/U ratios of 0.23–1.60. The sample XT contains seventeen detrital zircons ranging from 266 Ma to 492 Ma, with Th/U ratios of 0.38–2.27, reflecting a magmatic origin. The detailed CL images show that these zircons are mainly characterized by angular shapes and few zircons show sub-rounded shapes. Additionally, most of zircons have clear oscillatory zoning textures, and few zircons (dated at 291 Ma and 317 Ma) have no oscillatory zoning textures characterized by homogeneous textures. One detrital zircon (two analyses) dated at 490–492 Ma belongs to the Late Cambrian of the Early Paleozoic.

It is well-known that Paleozoic magmatism is insignificant in the western Shandong province and its peripheral areas (e.g., Xie et al., 2012; Li et al., 2013; Xu et al., 2013). Although Liu et al. (2006) reported a magnetite-amphibolite intrusion that was dated at 484–450 Ma in the western Shandong, our results are inconsistent with the magnetite-amphibolite intrusion. According to age populations and Hf isotopic features, Xu et al. (2013) concluded that there was an evident mountain or provenance region along the norther margin of the NCC during the Early to Late Jurassic, resulting in clastic materials southward into the hinterland of the NCC, such as the western Shandong province. Some researchers reported that there was an early Paleozoic magmatic event in the Sulu orogenic belt ranging from 346 to 500 Ma (e.g., Yang et al., 2003; Yang J. S. et al., 2005; Yang et al., 2009; Liu and Liou, 2011). This inferred that the Sulu orogenic belt might be the potential source for the Paleozoic zircon grains extracted from the Santai Formation of the western Shandong. In this study, the Early Paleozoic detrital zircons are derived from the western Shandong ranging from 419 to 492 Ma, whereas the sample JN collected from the Tanlu fault zone has no finding of the Early Paleozoic detrital zircons. This indicates that the Sulu orogenic belt cannot be a Paleozoic supplier for the basins formed in the western Shandong province. Furthermore, Xie et al. (2012) refuted the above arguments and pointed out that the Early Paleozoic arc magmatism might have not developed in the Sulu belt. Based on the spatial-temporal features, we argue that the Early Paleozoic detrital zircons cannot be derived from the Sulu orogenic belt.

As shown above, the Early Paleozoic magmatic events are scarce in the NCC; there was only an Early Paleozoic island arc belt (Bai-nai-miao island arc belt) that developed extensive arc-type and back-arc magmatic rocks in the norther margin of the NCC during the Middle Cambrian-Late Silurian (509–421 Ma) (e.g., Jian et al., 2008; Liu et al., 2014; Wu et al., 2016). In addition,

Zhang et al. (2011) reported the Cenozoic basalts that contained Early Paleozoic magmatic zircons (487–419 Ma) in the eastern Liaoning, suggesting that there were probably extensive magmatic events in the eastern Liaoning during the Early Paleozoic. Based on the temporal and genetic relationships, we conclude that the Early Paleozoic detrital zircons might be originated from the northern margin of the eastern NCC and the eastern Liaoning. Therefore, we conclude that several Early Paleozoic detrital zircons might have originated from the northern margin of the NCC or the eastern Liaoning in this study.

It has been proved that there was a Late Paleozoic Andean-style continental arc in the Inner Mongolia Paleo-uplift, which underwent large-scale exhumation and uplift during the Late Carboniferous to Early Jurassic due to the Paleo-Asian Ocean subduction (Zhang et al., 2007a; Zhang et al., 2007b; Xu et al., 2013). Therefore, the Inner Mongolia Paleo-uplift might provide detritus to the depositional basins for the hinterland of eastern NCC (e.g., Cope et al., 2005; Yang et al., 2006; Li et al., 2009, 2010; Xu et al., 2013). Subsequently, the collision of the NCC and Yangtze terrane resulted in the entire uplift of the eastern NCC, leading to the extensive denudation of the Upper Triassic strata during the Late Triassic. Until to the Early-Middle Jurassic, the collision of the Siberia and NCC-Mongolian plates resulted in the intense uplift of the Xing-Meng orogenic belt. Consequently, the Xing-Meng orogenic belt might be the main provenances for the depositional basins in the eastern NCC, and depositional peak in the Late Jurassic and ceased in the Latest Jurassic to the Earliest Cretaceous owing to the rapid uplift of the Yinshan-Yanshan orogenic belt forming a natural barrier (e.g., Yang et al., 2006; Xie et al., 2012; Xu et al., 2013). In addition, the Late Paleozoic magmatic events mainly occurred in the northern part of the NCC evidence from the SHRIMP and LA-ICP-MS U-Pb dating on the felsic intrusive rocks, volcanic tuff and mafic rocks, whose formation timing range from 395 Ma to 271 Ma (e.g., Zhang et al., 2007a; Zhang et al., 2007b; Zhang et al., 2009a; Zhang et al., 2009b; Zhang et al., 2009c). As stated above, the Late Paleozoic magmatic activities of the western Shandong province are not found and its peripheral areas, but the age populations of the detrital zircons from the Santai Formation in this study are well compared with that of the Xing-Meng orogenic belt and the northern part of the NCC. On the contrary, twelve Late Paleozoic detrital zircons of the sample JN were probably derived from the Yinshan-Yanshan orogenic belt (Li et al., 2013).

5.2.5 Mesozoic detrital zircons

5.2.5.1 Triassic detrital zircons

The sample JGZ contains eight Triassic zircon grains varying from 220 Ma to 251 Ma, with Th/U ratios of 0.59–2.23, indicating a magmatic origin (Corfu et al., 2003). These Triassic detrital zircons are mostly characterized by euhedral, suggesting a near-by magmatic provenance (Corfu et al., 2003). The sample ZRL contains four Triassic detrital zircons ranging

from 210 Ma to 247 Ma. The four detrital zircons have Th/U ratios of 0.44–1.27, reflecting a magmatic origin. In the CL images, these detrital zircons have angular shapes and clear oscillatory zoning, suggesting a near-by depositional provenance. The sample JN contains five Triassic detrital zircons from 233 Ma to 248 Ma, with Th/U ratios of 0.49–1.15, reflecting a magmatic origin. Additionally, these zircons show sub-rounded to angular shapes with weak oscillatory zoning. Besides one detrital zircon, the other detrital zircons are grey-black color. The sample XT contains nine Triassic detrital zircons ranging from 221 Ma to 247 Ma, with Th/U ratios of 0.46–2.24, corresponding to a magmatic origin. The three detrital zircons dated at 221 Ma, 240 Ma and 241 Ma, have complicated textures characterized by a core rimmed by a new overgrowth rim, indicating a complicated geological process. The others show angular shapes with clear oscillatory zoning textures. The Sulu orogenic belt is characterized by the Triassic UHP metamorphism (dating the zircon grain rim) and develops a few Late Triassic intrusions in the southeastern edge. In addition to the Sulu orogenic belt, the Yinshan-Yanshan orogenic belt developed Phanerozoic igneous zircons ranging from 415 to 107 Ma (e.g., Zheng et al., 2004; Tian et al., 2007; Zhang et al., 2007a; Zhang et al., 2007b; Ma and Zheng, 2009; Zhang et al., 2009a; Zhang et al., 2009b; Shi et al., 2010). Compared to the Yinshan-Yanshan orogenic belt, the zircons, derived from the Sulu belt, have low Th/U ratios and metamorphic genesis (Xie et al., 2012). In addition, the zircons are derived from the Sulu orogenic belt, which shows the age clusters concentrating on the Late Triassic. Furthermore, the detrital zircons extracted from the Sulu belt have complicated CL textures characterized by inhomogeneous and core-rim structures. During the Early Jurassic to Early Cretaceous, the Tanlu fault zone could have served as a potential barrier to prohibit the detritus from the Sulu belt due to the large-scale sinistral strike-slip movement. Based on the CL images and age clusters as well as tectonic setting, we argue that the Triassic detrital zircons were predominantly from the Yinshan-Yanshan orogenic belt, and few zircons (sample XT) consistent with the timing of the UHP metamorphism (245–218 Ma) and retrograde metamorphism of amphibolite facies might be derived from the Sulu orogenic belt (Liu F. L. et al., 2009). Compared to the Yinshan-Yanshan provenance, the Triassic detrital zircons sourced from the Sulu orogenic belt have complicated textures and clear over-growth rim.

5.3.5.2 Jurassic to Early Cretaceous detrital zircons

The sample JGZ contains eight Jurassic detrital zircons ranging from 153 Ma to 178 Ma. These zircons have high Th/U ratios of 0.58–1.35 and angular shapes with oscillatory zoning textures, suggesting a magmatic origin and near-by depositional setting. The sample ZRL contains three Jurassic detrital zircons dated at 149 Ma, 151 Ma and 195 Ma, with Th/U ratios of 0.62–2.03, reflecting a magmatic origin. The Late Jurassic

zircons (149 Ma and 151 Ma) both show angular shapes and clear oscillatory zoning, whereas the zircon dated at 195 Ma show clear core-rim texture, and core shows grey-dark color revealing a metamorphism (high U content). The rim of the Early Jurassic zircon shows grey color and has high Th/U ratio of 0.62 and oscillatory zoning, reflecting a magmatic origin. The sample JN contains four Jurassic detrital zircons ranging from 152 Ma to 180 Ma. These zircons have high Th/U ratios of 0.66–1.75 (>0.4) and oscillatory zoning, suggesting a magmatic origin. Compared to the Jurassic detrital zircons, the sample JN has an overwhelming majority of the Early Cretaceous detrital zircons ranging from 120 Ma to 139 Ma (total=34), with a peak age at circa 125 Ma (Figure 10C). These Early Cretaceous detrital zircons have high Th/U ratios of 0.39–2.57 and most of them show angular morphologies and oscillatory zoning textures, suggesting a magmatic origin and near-by depositional setting. In addition, the CL images show that these Early Cretaceous detrital zircons have typical oscillatory zoning textures rather than tabular zoning, indicating that the detrital zircons might be sourced from the intermediate-felsic rocks. The sample XT contains six Jurassic detrital zircons ranging from 147 Ma to 168 Ma, with high Th/U ratios of 0.41–1.40 (>0.4), suggesting a magmatic origin. In addition, these zircons recovered from the sample XT show clear oscillatory zoning and angular shapes, reflecting a near-by depositional setting as well.

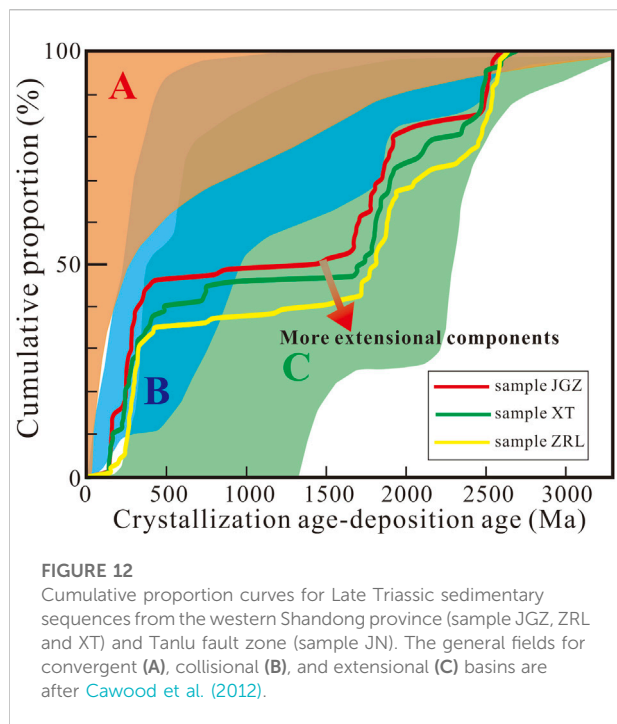
The Jurassic magmatism occurred in the western and eastern Shandong province (e.g., Lin et al., 1996; Miao et al., 1997; Wang et al., 1998; Yang et al., 2005a; Guo et al., 2005; Shao et al., 2007; Zhang et al., 2010; Zhang et al., 2011; Lan et al., 2012; Zhang et al., 2012; Xu et al., 2016). Xu et al. (2015) proposed that the western Shandong region had no obvious provenance connection with the Sulu orogenic belt during the Jurassic to Early Cretaceous due to the natural barrier of the Tanlu fault zone. Therefore, we also consider that the Sulu orogenic belt play an insignificant role contributing the depositional detritus to the depositional basins/depressions in the western Shandong. In this study, we argued that the Jurassic detrital zircons of the Santai Formation mostly are mainly derived from the western Shandong province, and one detrital zircon characterized by clear core-rim texture is probably derived from the Sulu orogenic belt, which is associated exhumation of the post-collisional magmatism (Xu et al., 2016).

The Cretaceous magmatic events are widespread in the whole Sulu orogenic belt and Jiaobei terrane. In the Jiaobei terrane, the Guojialing granitoid batholiths were formed at 120–135 Ma (e.g., Li et al., 2018). According to the Al-in-hornblende barometry, the Guojialing granitoid batholiths were formed under the pressures of 3.2–5.4 kbar similar to 12 km emplacement depth (Li et al., 2018). Therefore, the Guojialing granitoid batholiths could not be exhumed to the surface at ca. 120 Ma. Thus, the 120–130 Ma detrital zircons are not derived from the Guojialing granitoid batholiths. In addition to the Jiaobei terrane, the Sulu orogenic belt developed extensive Early Cretaceous magmatic

events (e.g., Zhang et al., 2010, 2012; Meng et al., 2018). Based on the geobarometer and paleogeography, granitic plutons in the Sulu belt had a relatively deep emplacement depth from ca. 9–11 km (e.g., Wang et al., 2016; Meng et al., 2020), indicating that the Early Cretaceous granitic plutons could not be a supplier for the rifted basins in the Tanlu fault zone. Although Lin et al. (2005) and Liu S. S. et al. (2009) proposed that the Sulu terrane experienced quick uplift between 130 Ma and 100 Ma, large-scale denudation and significant uplift began in the early Late Cretaceous rather than the middle Early Cretaceous. According to dinosaur tracks and youngest detrital zircons (Figure 11C), the sedimentary basin was formed at ca. 122 Ma in the Tanlu fault zone; thus, the coeval granitoid rocks cannot provide denudated materials to the near-by fault basins. According to the regional geology and rock assemblages, we argue that the Early Cretaceous granitic batholiths of the Sulu belt were exhumed to the surface and eroded significantly during the early Late Cretaceous. Zhang et al. (2016) concluded that there were extensive coastal mountains during the early Late Cretaceous in the eastern China. We agree with Zhang et al. (2016) that large-scale denudation of the Early Cretaceous granitoid batholiths occurred in the early Late Cretaceous in the Sulu orogenic belt rather than the middle Early Cretaceous (equivalent emplacement timing). In addition, the Mesozoic detrital zircons are predominant, displaying the similar unimodal age spectra clustering around 120 Ma to 257 Ma (peak age at 125 Ma) (Figure 10C). The Mesozoic detrital zircons have an overwhelming advantage implying a near-by volcanic depositional environment. The eastern Shandong developed extensive volcano-magmatic events of the Qingshan period during the Early Cretaceous. Therefore, the Early Cretaceous volcanic and subvolcanic rocks might be the best supplier for the basins in the Tanlu fault zone, corresponding to a near-by volcanic depositional setting. Combined with paleogeography and the emplacement depth of Mesozoic granites in the Jiaodong Peninsula (e.g., Wang et al., 2016; Li et al., 2018), we consider that the Early Cretaceous zircons, which have high Th/U ratios and angular shapes, were derived from coeval volcanic and subvolcanic rocks of the Qingshan period rather than coeval intrusive granitic plutons, such as granites from the Jiaobei and the Sulu orogenic belt.

5.3 Tectonic setting and implications

It has been proved that the eastern NCC had a high relief without deposition due to the collision of the Yangtze and NCC during the Late Triassic to Early Jurassic (e.g., Wu et al., 2007; Li and Huang, 2013). However, the paleogeomorphology of the hinterland of the eastern NCC had changed significantly during the late Early Jurassic to the Valanginian of the Early Cretaceous (180–136 Ma) (e.g., Xu and Li, 2015). For example, the Fangzi, Santai and Mengyin formations had received a mass of depositional loads from the



northern part of the NCC and Xing-Meng orogenic belt. This indicates that the northern NCC and Xing-Meng orogenic belt might be the predominant depositional source region for the hinterland of the eastern NCC, which lasted the Valanginian stage of the Early Cretaceous (~136 Ma). Consequently, the northern NCC and the Xing-Meng orogenic belt, which underwent quick uplifting and denudation during the Bathonian stage of the Middle Jurassic, are the joint source regions for the Early-Middle Jurassic sediments in the western Shandong province and adjacent regions. Subsequently, the northern NCC contributed more Early Cretaceous detrital materials to the western Shandong Province than the Xing-Meng orogenic belt during the middle Early Cretaceous (Graham et al., 2001; Wang et al., 2012; Xu and Li, 2015).

Cawood et al. (2012) proposed that age spectra of detrital zircons can reflect their formational environment of the basins in which they are deposited. Different sedimentary environments show different age clusters of detrital zircons. Generally, sediments deposited in the convergent plate margins are characterized by a large proportion of zircon ages close to their depositional age, while the sediments deposited in the intracratonic, extensional and collisional settings contain greater proportions with older ages, which reflect the history of the underlying basement (Cawood et al., 2012). If the sediments are deposited in a region with absence of coeval magmatism, the detrital zircons would be not useful in constraining the depositional age of the basins. In the western Shandong and the Tanlu fault zone regions, in addition to the Precambrian volcano-magmatic and metamorphic events, Mesozoic magmatic events are widespread throughout in the

whole Shandong province of the eastern NCC (e.g., Xu et al., 2004; Yang et al., 2012; Yang et al., 2013; Yang et al., 2021). Therefore, formational timing of the Late Mesozoic sedimentary basins in the western Shandong province and adjacent regions can be constrained well by detrital zircons.

In the cumulative proportion plot (Figure 12), the samples collected from the western Shandong province (JGZ, ZRL and XT) show similar distribution patterns with those derived from the extensional basins, indicating an extensional setting. Interestingly, the results for the Santai Formation have shown that more and more extensional components were preserved in the strata from the lowermost (sample JGZ) to the uppermost part (sample ZRL), indicating an extensional process gradually (Figure 12). Compared to the Early Cretaceous, the Late Jurassic tectonic setting and tectonic framework of the eastern NCC remain enigmatic during the Jurassic (Yang et al., 2021), which might be associated with the large-scale sinistral strike-slip of the Tanlu Fault and the subduction of the Paleo-pacific ocean lithosphere. In the eastern NCC, the Early-Middle Jurassic granitoid rocks (intermediate-acidic rocks) are characterized by low crystallization temperatures and adakite-like chemical features, indicating a significant crustal thickening (compressional continental arc setting) (Liu et al., 2010; Liu et al., 2013). By contrast, the Late Jurassic is a key tectonic transition in the eastern NCC evidenced by the 160–140 Ma magmatic rocks. Although the tectonic transition was documented well within the magmatic rocks, the information of the extensional tectonics is poorly constrained or reported in sedimentary rocks. In this study, our samples from the Santai Formation plot into the extensional setting, indicating that the extension of the upper crust might occur during the Late Jurassic in the western Shandong province of the eastern NCC. The upper crustal extension might be the shallow response of the NCC destruction. In addition to the magmatic and sedimentary clues, the metamorphic core complexes (MCC), the most representative extensional tectonic assemblages, are the thinning and destruction products of the lithospheric mantle, reflecting the shallow responses of the upper crustal extension (e.g., Ni et al., 2013; Ni et al., 2016; Xia et al., 2016). Therefore, the accurate formation timing of the MCC can give better constraints on the destruction and thinning of the eastern NCC. The published data show that the MMC were formed during the 150–121 in the eastern NCC, and peak at 125 Ma (e.g., Xia et al., 2016). Consequently, we argue that the basins deposited in the Late Jurassic might be the extensional products of the Shandong province in the eastern NCC. The Santai Formation was deposited in an extensional setting, and potentially is the shallow response of the eastern NCC destruction. It has been well-recognized that the eastern NCC experienced large-scale lithospheric thinning during the Late Mesozoic, especially the Early Cretaceous (destruction peaking at circa 125 Ma). Thus, the sample JN was deposited in the Early Cretaceous (ca. 122 Ma) that was combined product of the sinistral strike-slip of the Tanlu Fault and large-scale extension of the lithosphere of the eastern NCC.

6 Conclusion

Comparing the detrital zircon U-Pb ages, zircon morphologies and trace elemental features of the Late Mesozoic sedimentary rocks from the western Shandong province and Tanlu fault zone, we conclude the following:

- 1) Late Triassic and Neoproterozoic detrital zircons play a minor role in the sedimentary strata of the western Shandong province, indicating that the Tanlu fault zone has served as a natural “barrier” characterized by the graben-horst-graben structures preventing detritus of the Sulu orogenic belt.
- 2) The samples collected from the western Shandong and Tanlu fault zone have different age clusters, suggesting that the large sinistral movement of the Tanlu fault zone might have occurred at the Early-Middle Jurassic and formed a paleogeographic separation of the western Shandong and eastern Shandong (Sulu orogenic belt).
- 3) The Santai Formation had begun deposition at circa 158 Ma and probably had terminated deposition at circa 150 Ma as evidenced by the weighted average ages of the youngest zircons from the lowermost and uppermost parts of the Santai Formation. The Tianjialou Formation of the Dasheng Group characterized by the dinosaur and bird tracks had begun deposition at circa 122 Ma as evidenced by the weighted average ages of the youngest zircons.
- 4) U-Pb ages of detrital zircons from the western Shandong province reveal three major age groups 2,475–2,540 Ma, 1820–1870 Ma and 257–285 Ma, with minor Mesoproterozoic, Neoproterozoic and Paleozoic detrital zircons.
- 5) According to detrital zircon age populations and features of the depositional provenance, the sediments deposited in the western Shandong province are mainly sourced from the basement uplift of the western Shandong province (Late Neoproterozoic to Earliest Paleoproterozoic detrital zircons), the Jiao-Liao Belt (Orosirian stage detrital zircons of the Paleoproterozoic), northern part of the NCC and Xing-Meng orogenic belt (Late Paleoproterozoic detrital zircons). The sample JN deposited in the Tanlu fault zone is mainly derived from the volcanic and subvolcanic rocks of the Qingshan period in the eastern Shandong, and the Jiao-Liao and the uplift of the western Shandong are the subordinate depositional source, with minor supplier being derived from the Yinshan-Yanshan orogenic belt.
- 6) Evidence from the Late Jurassic sediments in the western Shandong province indicate that the extension and thinning of the NCC lithosphere might begin at ca. 158 Ma.

Data availability statement

The original contributions presented in the study are included in the article/[Supplementary Material](#), further inquiries can be directed to the corresponding author.

Author contributions

YM wrote and edited this paper; HY edited this paper and draw pictures; QW edited this paper and field sampling; FM polished and edited this paper; XR draw pictures and data processing.

Funding

This study was co-supported by the Key Laboratory of Deep-Earth Dynamics of Ministry of Natural Resources (J1901-16), Key Laboratory of Gold Mineralization Processes and Resource Utilization (MNR) and Shandong Provincial Key Laboratory of Metallogenic Geological Process and Resource Utilization (Kfkt202103), and the Young Innovative Projects of Shandong Province (2019KJH004).

Acknowledgments

We would like to express our gratitude to the Editor and reviewers for their insightful comments, which helped considerably in improving the manuscript. First author thanks Rihui Li for his academic guidance, and this paper is dedicated to Rihui Li for his contributions to the Paleocology and Paleontology. We are grateful to Bangqi Liang for his field guidance and sampling.

Conflict of interest

The authors declare that the research was conducted in the absence of any commercial or financial relationships that could be construed as a potential conflict of interest.

Publisher's note

All claims expressed in this article are solely those of the authors and do not necessarily represent those of their affiliated organizations, or those of the publisher, the editors and the reviewers. Any product that may be evaluated in this article, or claim that may be made by its manufacturer, is not guaranteed or endorsed by the publisher.

Supplementary material

The Supplementary Material for this article can be found online at: <https://www.frontiersin.org/articles/10.3389/feart.2022.995848/full#supplementary-material>

References

- Andersen, T. (2005). Detrital zircons as tracers of sedimentary provenance: limiting conditions from statistics and numerical simulation. *Chem. Geol.* 216, 249–270. doi:10.1016/j.chemgeo.2004.11.013
- Ballard, J. R., Palin, J. M., Williams, I. S., Campbell, I. H., and Faunes, A. (2001). Two ages of porphyry intrusion resolved for the super-giant Chuquibambilla copper deposit of northern Chile by ELA-ICP-MS and SHRIMP. *Geol.* 29, 383–386. doi:10.1130/0091-7613(2001)029<0383:taopir>2.0.co;2
- BGMRS (Bureau of Geology and Mineral Resources of Shandong Province) (1991). *Regional geology of Shandong province*. Beijing: Geological Publishing House, 1–595. (in Chinese with English abstract).
- Boynnton, W. V. (1984). “Cosmochemistry of the rare Earth elements: Meteorite studies,” in *Rare earth elements geochemistry*. Editor P. Henderson (Amsterdam: Elsevier), 63–114.
- Cawood, P. A., Hawkesworth, C. J., and Dhuime, B. (2012). Detrital zircon record and tectonic setting. *Geology* 40 (10), 875–878. doi:10.1130/g32945.1
- Chang, Z. S., Vervoort, J. D., McClelland, W. C., and Knaack, C. (2006). U-Pb dating of zircon by LA-ICP-MS. *Geochem. Geophys. Geosyst.* 7 (5), Q05009. doi:10.1029/2005gc001100
- Cope, T. D., Ritts, B. D., Darby, B. J., Fildani, A., and Graham, S. A. (2005). Late paleozoic sedimentation on the northern margin of the north China block: implications for regional tectonics and climate change. *Int. Geol. Rev.* 47, 270–296. doi:10.2747/0020-6814.47.3.270
- Corfu, F., Hancher, J. M., Hoskin, P. W., and Kinny, P. (2003). Atlas of zircon textures. *Rev. Mineralogy Geochem.* 53 (1), 469–500. doi:10.2113/0530469
- Dickinson, W. R., and Gehrels, G. E. (2009). Use of U-Pb ages of detrital zircons to infer maximum depositional ages of strata: A test against a Colorado Plateau Mesozoic database. *Earth Planet. Sci. Lett.* 288, 115–125. doi:10.1016/j.epsl.2009.09.013
- Fedo, C. M., Sircombe, C. M., and Rainbird, R. H. (2003). Detrital zircon analysis of the sedimentary record. *Rev. Mineral. Geochem.* 53, 277–303. doi:10.2113/0530277
- Gao, S., Rudnick, R. L., Yuan, H. L., Liu, X. M., Liu, Y. S., Xu, W. L., et al. (2004). Recycling lower continental crust in the North China craton. *Nature* 432, 892–897. doi:10.1038/nature03162
- Gehrels, G. (2014). Detrital zircon U-Pb geochronology applied to tectonics. *Annu. Rev. Earth Planet. Sci.* 42, 127–149. doi:10.1146/annurev-earth-050212-124012
- Graham, S. A., Hendrix, M. S., Johnson, C. L., Badamgarav, D., Badarch, G., Amory, J., et al. (2001). Sedimentary record and tectonic implications of Mesozoic rifting in southeast Mongolia. *Geol. Soc. Am. Bull.* 113, 1560–1579. doi:10.1130/0016-7606(2001)113<1560:rsatio>2.0.co;2
- Guo, J. H., Chen, F. K., Zhang, X. M., Siebel, W., and Zhai, M. G. (2005). Evolution of syn- to post-collisional magmatism from north Sulu UHP belt, eastern China: zircon U-Pb geochronology. *Acta Petrol. Sin.* 21 (4), 1281–1301. (in Chinese with English abstract) doi:10.3321/j.issn:1000-0569.2005.04.025
- Hacker, B. R., Ratschbacher, L., Webb, L., Ireland, T., Walker, D., and Dong, S. W. (1998). U/Pb zircon ages constrain the architecture of the ultrahigh-pressure Qinling-Dabie Orogen, China. *Earth Planet. Sci. Lett.* 161, 215–230. doi:10.1016/s0012-821x(98)00152-6
- Hoskin, P. W. O., and Ireland, T. R. (2000). Rare Earth element chemistry of zircon and its use as a provenance indicator. *Geology* 28, 627–630. doi:10.1130/0091-7613(2000)028<0627:reecoz>2.3.co;2
- Jahn, B., Auvray, B., Shen, Q., Liu, D., Zhang, Z., Dong, Y., et al. (1988). Archean crustal evolution in China: The Taishan complex, and evidence for juvenile crustal addition from long-term depleted mantle. *Precambrian Res.* 38, 381–403. doi:10.1016/0301-9268(88)90035-6
- Jahn, B., Liu, D., Wan, Y., Song, B., and Wu, J. (2008). Archean crustal Evolution of the Jiaodong Peninsula, China, as revealed by zircon SHRIMP geochronology, elemental and Nd isotope geochemistry. *Am. J. Sci.* 308 (3), 232–269. doi:10.2475/03.2008.03
- Jian, P., Liu, D. Y., Kröner, A., Windley, B. F., Shi, Y., Zhang, F., et al. (2008). Time scale of an early to mid-Paleozoic orogenic cycle of the long-lived Central Asian Orogenic Belt, Inner Mongolia of China: Implications for continental growth. *Lithos* 101 (3–4), 233–259. doi:10.1016/j.lithos.2007.07.005
- Lan, T. G., Fan, H. R., Santosh, M., Hu, F. F., Yang, K. F., Yang, Y. H., et al. (2012). Early jurassic high-K calc-alkaline and shoshonitic rocks from the Tongshi intrusive complex, Eastern North China craton: implication for crust-mantle interaction and post-collisional magmatism. *Lithos* 140–141, 183–199. doi:10.1016/j.lithos.2012.01.015
- Li, H. Y., and Huang, X. L. (2013). Constraints on the paleogeographic evolution of the north China craton during the late triassic-jurassic. *J. Asian Earth Sci.* 70 (71), 308–320. doi:10.1016/j.jseas.2013.03.028
- Li, R. H., Liu, M. W., and Songchuan, Z. S. (2002). Discovery of jurassic dinosaur track in Shandong. *Geol. Bull. China* 21 (8–9), 596–597. (in Chinese).
- Li, R. H., Liu, M. W., and Lockley, M. R. (2005a). Early cretaceous dinosaur tracks from the houzuoshan dinosaur park in junan county, Shandong province, China. *Geol. Bull. China* 24 (3), 277–226. (in Chinese with English abstract).
- Li, R. H., Lockley, M. G., and Liu, M. W. (2005b). A new ichnotaxon of fossil bird track from the early cretaceous Tianjialou formation (Barremian-Albian), Shandong province, China. *Chin. Sci. Bull.* 50 (11), 1149–1154. (in Chinese). doi:10.1360/982004-823
- Li, Z., Li, Y., Zheng, J. P., and Han, D. (2007). Late mesozoic tectonic transition of the Eastern North China craton: Evidence from basin-fill records. *Geol. Soc. Lond. Spec. Publ.* 280, 239–265. doi:10.1144/sp280.12
- Li, H. Y., Xu, Y. G., Huang, X. L., He, B., and Yan, B. (2009). Activation of northern margin of the north China craton in late paleozoic: Evidence from U-Pb dating and Hf isotopes of detrital zircons from the upper carboniferous Taiyuan Formation in the ningwu-jingle basin. *Chin. Sci. Bull.* 54, 677–686. doi:10.1007/s11434-008-0444-9
- Li, S. J., He, M., Yang, B., Chen, F. B., and Yao, Q. H. (2010). The division and correlation of the Mesozoic stratigraphic subregions in Shandong province. *J. Stratigr.* 34 (2), 167–172. (in Chinese with English abstract).
- Li, H. Y., Xu, Y. G., Liu, Y. M., Huang, X. L., and He, B. (2013). Detrital zircons reveal no Jurassic plateau in the eastern North China Craton. *Gondwana Res.* 24, 622–634. doi:10.1016/j.gr.2012.12.007
- Li, R. H., Liu, M. W., and Du, S. X. (2015). Dinosaur tracks from middle-upper jurassic Santai Formation: New materials and new interpretation. *Shandong Land Resour.* 31 (7), 1–3. (in Chinese with English abstract).
- Li, X. H., Fan, H. R., Zhang, Y. W., Hu, F. F., Yang, K. F., Liu, X., et al. (2018). Rapid exhumation of the northern Jiaobei terrane, north China craton in the early cretaceous: Insights from Al-in-hornblende barometry and U-Pb geochronology. *J. Asian Earth Sci.* 160, 365–379. doi:10.1016/j.jseas.2017.10.001
- Lin, J. Q., Tan, D. J., and Jin, Y. (1996). ⁴⁰Ar/³⁹Ar ages of Mesozoic igneous activities in Western Shandong. *Acta Pet. Mineral.* 15 (3), 213–220. (in Chinese with English abstract).
- Lin, L. H., Wang, P. L., Lo, C. H., Tsai, C. H., and Jahn, B. (2005). ⁴⁰Ar-³⁹Ar thermo chronological constraints on the exhumation of ultrahigh-pressure metamorphic rocks in the Sulu terrane of eastern China. *Int. Geol. Rev.* 47, 872–886. doi:10.2747/0020-6814.47.8.872
- Liu, F. L., and Liou, J. G. (2011). Zircon as the best mineral for P-T-time history of UHP metamorphism: a review on mineral inclusions and U-Pb SHRIMP ages of zircons from the dabie-sulu UHP rocks. *J. Asian Earth Sci.* 40, 1–39. doi:10.1016/j.jseas.2010.08.007
- Liu, C. H., and Liu, F. L. (2015). The mesoproterozoic rifting in the north China craton: A case study for magmatism and sedimentation of the zhaertai-bayan obo-Huade rift zone. *Acta Petrol. Sin.* 31 (10), 3107–3128.
- Liu, J. M., Yang, C. H., Yang, D. B., Xu, W. L., Wang, W. D., and Liu, J. T. (2006). U-Pb chronology in zircon of magnetite-amphibolite intrusion from Western Shandong and its geological implications. *Glob. Geol.* 25, 221–228. (in Chinese with English abstract).
- Liu, F. L., Gerdes, A., and Xue, H. M. (2009a). Differential subduction and exhumation of crustal slices in the Sulu HP-UHP metamorphic terrane: insights from mineral inclusions, trace elements, U-Pb and Lu-Hf isotope analyses of zircon in orthogneiss. *J. Metamorph. Geol.* 27 (9), 805–825. doi:10.1111/j.1525-1314.2009.00833.x
- Liu, S. S., Glasmacher, U., Xu, Z. Q., Weber, U., Wagner, G., Jonckheere, R., et al. (2009b). Thermotectonic history of Sulu UHP metamorphic rock: apatite fission track constraints from MH and PP2 of CCSD. *Acta Petrol. Sin.* 25, 1612–1618.
- Liu, S. F., Zhang, J. F., Hong, S. Y., and Ritts, B. D. (2010). Early Mesozoic basin development and its response to thrusting in the Yanshan Fold-and-Thrust belt, China. *Int. Geol. Rev.* 49, 1025–1049. doi:10.2747/0020-6814.49.11.1025
- Liu, S. F., Su, S., and Zhang, G. W. (2013). Early Mesozoic basin development in North China: Indications of cratonic deformation. *J. Asian Earth Sci.* 62, 221–236. doi:10.1016/j.jseas.2012.09.011
- Liu, C. F., Liu, W. C., Wang, H. P., Zhou, Z. G., Zhang, H. F., and Tang, Y. J. (2014). Geochronology and geochemistry of the Bainaimiao metavolcanic rocks in the northern margin of north China craton. *Acta Geol. Sin.* 88 (7), 1273–1287. (in Chinese with English abstract).

- Ludwig, K. R. (2003). *User's manual for Isoplot 3.0: A geochronological toolkit for Microsoft Excel*. Berkeley Calif: Berkeley Geochronology Center.
- Luo, Y., Sun, M., Zhao, G. C., Li, S., Ayers, J. C., Xia, X., et al. (2008). A comparison of U-Pb and Hf isotopic compositions of detrital zircons from the north and South Liaohe groups: Constraints on the evolution of the jiao-liao-ji belt, north China craton. *Precambrian Res.* 163 (3-4), 279–306. doi:10.1016/j.precamres.2008.01.002
- Ma, Q., and Zheng, J. P. (2009). *In-situ* U–Pb dating and Hf isotopic analyses of zircons in the volcanic rock of the Lanqi Formation in the Beipiao area, Western Liaoning Province. *Acta Petrol. Sin.* 25 (12), 3287–3297.
- Meng, Y. K., Santosh, M., Li, R. H., Xu, Y., and Hou, F. H. (2018). Petrogenesis and tectonic implications of early cretaceous volcanic rocks from lingshan island in the Sulu orogenic belt. *Lithos* 312–313, 244–257. doi:10.1016/j.lithos.2018.05.009
- Meng, Y. K., Wang, Z. B., Gan, B. P., and Liu, J. Q. (2020). Petrogenesis and tectonic implications of the early cretaceous granitic pluton in the Sulu orogenic belt: The Caochang granitic pluton as an example. *Minerals* 10 (5), 432. doi:10.3390/min10050432
- Menzies, M. A., Fan, W. M., and Zhang, M. (1993). "Palaeozoic and Cenozoic lithoprobe and the loss of >120 km of Archean lithosphere, Sino-Korean craton, China," in *Magmatic processes and Plate tectonic*. Editors H. M. Prichard, T. Alabaster, N. B. W. Harris, and C. R. Neary (London: Geological Society, Special Publication), 76, 71–81.
- Miao, L., Luo, Z., Huang, J., Guan, K., McNaughton, N. J., Groves, D. I., et al. (1997). Zircon sensitive high resolution ion microprobe (SHRIMP) study of granitoid intrusions in Zhaoye gold belt of Shandong province and its implication. *Sci. China Ser. D-Earth. Sci.* 40 (4), 361–369. doi:10.1007/bf02877567
- Nelson, D. R. (2001). An assessment of the determination of depositional ages for Precambrian clastic sedimentary rocks by U–Pb dating of detrital zircons. *Sediment. Geol.* 141 (142), 37–60. doi:10.1016/s0037-0738(01)00067-7
- Ni, J., Liu, J., Tang, X., Yang, H., Xia, Z., and Guo, Q. (2013). The wulian metamorphic core complex: A newly discovered metamorphic core complex along the Sulu orogenic belt, eastern China. *J. Earth Sci.* 24 (3), 297–313. doi:10.1007/s12583-013-0330-5
- Ni, J., Liu, J., Tang, X., Yang, H., Xia, Z., and Zhang, T. (2016). Early Cretaceous exhumation of the Sulu orogenic belt as a consequence of the eastern Eurasian tectonic extension: Insights from the newly discovered Wulian metamorphic core complex, eastern China. *J. Geol. Soc. Lond.* 173 (3), 531–549. doi:10.1144/jgs2014-122
- Peng, P., Bleeker, W., Ernst, R. E., Söderlund, U., and McNicoll, V. (2011a). U-Pb baddeleyite ages, distribution and geochemistry of 925 Ma mafic dykes and 900 Ma sills in the north China craton: Evidence for a neoproterozoic mantle plume. *Lithos* 127, 210–221. doi:10.1016/j.lithos.2011.08.018
- Peng, P., Zhai, M. G., Li, Q. L., Wu, F. Y., Hou, Q. L., Li, Z., et al. (2011b). Neoproterozoic (~900Ma) Sariwon sills in North Korea: Geochronology, geochemistry and implications for the evolution of the south-eastern margin of the North China Craton. *Gondwana Res.* 20, 243–254. doi:10.1016/j.gr.2010.12.011
- Peng, T. P., Wilde, S. A., Fan, W. M., and Peng, B. X. (2013). Neoproterozoic high-Mg basalt (SHMB) from the taishan granite-greenstone terrane, eastern North China craton: petrogenesis and tectonic implications. *Precambrian Res.* 228, 233–249. doi:10.1016/j.precamres.2013.01.017
- Ren, P., Xie, H. Q., Wang, S. J., Nutman, A., Dong, C. Y., Liu, S. J., et al. (2016). A ca. 2.60 Ga tectono-thermal event in Western Shandong Province, North China Craton from zircon U-Pb isotopic evidence: Plume or convergent plate boundary process. *Precambrian Res.* 281, 236–252. doi:10.1016/j.precamres.2016.05.016
- Rubatto, D. (2017). Zircon: the metamorphic mineral. *Rev. Mineral. Geochem.* 83 (1), 261–295. doi:10.2138/rmg.2017.83.9
- SBGMR (Shandong Bureau of Geology and Mineral Resources) (2003). *Regional geology of Shandong province*. Jinan: Shandong Mapping Press. (in Chinese).
- Shao, J. A., Mu, B. L., and Zhang, L. Q. (2000). Deep geological process and its shallow response during Mesozoic transfer of tectonic frameworks in eastern North China. *Geol. Rev.* 46, 32–40. (in Chinese with English abstract). doi:10.16509/j.georeview.2000.01.006
- Shao, J. A., Zhang, H. F., Liu, X. M., and Li, Z. T. (2007). Chronological record of the early mesozoic underplating in the northern margin of north China: U-Pb chronometry of zircons in the late mesozoic andesite from West Liaoning province. *Prog. Nat. Sci.* 17 (4), 79–82. (in Chinese).
- Shi, Y. R., Liu, D. Y., Miao, L. C., Zhang, F. Q., Jian, P., Zhang, W., et al. (2010). Devonian A-type granitic magmatism on the northern margin of the north China craton: SHRIMP U–Pb zircon dating and Hf-isotopes of the hongshan granite at Chifeng, inner Mongolia, China. *Gondwana Res.* 17, 632–641. doi:10.1016/j.gr.2009.11.011
- Sircombe, K. N. (1999). Tracing provenance through the isotope ages of littoral and sedimentary detrital zircon, eastern Australia. *Sediment. Geol.* 124, 47–67. doi:10.1016/s0037-0738(98)00120-1
- Tam, P. Y., Zhao, G. C., Liu, F. L., Zhou, X., Sun, M., and Li, S. (2011). Timing of metamorphism in the paleoproterozoic jiao-liao-ji belt: New SHRIMP U-Pb zircon dating of Granulites, gneisses and Marbles of the Jiaobei Massif in the north China craton. *Gondwana Res.* 19 (1), 150–162. doi:10.1016/j.gr.2010.05.007
- Tang, J., Zheng, Y. F., Wu, Y. B., Gong, B., and Liu, X. M. (2008). Zircon U–Pb age and geochemical constraints on the tectonic affinity of the Jiaodong terrane in the Sulu orogen, China. *Precambrian Res.* 161, 389–418. doi:10.1016/j.precamres.2007.09.008
- Tian, W., Chen, B., Liu, C. Q., and Zhang, H. F. (2007). Zircon U–Pb age and Hf isotopic composition of the Xiaozhangjiakou ultramafic pluton in northern Hebei. *Acta Petrol. Sin.* 23, 583–590. (in Chinese with English abstract).
- Vermeesch, P. (2012). On the visualisation of detrital age distributions. *Chem. Geol.* 312–313, 190–194. doi:10.1016/j.chemgeo.2012.04.021
- Wan, Y. S., Liu, D. Y., Wang, S. J., Dong, C. Y., Yang, E. X., Wang, W., et al. (2010). Juvenile magmatism and crustal recycling at the end of the neoproterozoic in Western Shandong province, north China craton: Evidence from SHRIMP zircon dating. *Am. J. Sci.* 310, 1503–1552. doi:10.2475/10.2010.11
- Wan, Y. S., Liu, D. Y., Wang, S. J., Yang, E. X., Wang, W., Dong, C. Y., et al. (2011). ~2.7Ga juvenile crust formation in the North China Craton (Taishan-Xintai area, Western Shandong Province): Further evidence of an understated event from U–Pb dating and Hf isotopic composition of zircon. *Precambrian Res.* 186, 169–180. doi:10.1016/j.precamres.2011.01.015
- Wan, Y. S., Dong, C. Y., Liu, D. Y., Kröner, A., Yang, C. H., Wang, W., et al. (2012). Zircon ages and geochemistry of Late Neoproterozoic syenogranites in the North China Craton: A review. *Precambrian Res.* 222–223, 265–289. doi:10.1016/j.precamres.2011.05.001
- Wan, Y. S., Xie, H. Q., Dong, C. Y., and Liu, D. Y. (2020). Timing of tectonothermal events in archaic basement of the north China craton. *Earth Sci.* 45 (9), 3119–3160. (in Chinese with English abstract). doi:10.3799/dqkx.2020.121
- Wang, L. G., Qiu, Y. M., McNaughton, N. J., Groves, D. I., Luo, Z. K., Huang, J. Z., et al. (1998). Constraints on crustal evolution and gold metallogeny in the North Western Jiaodong Peninsula, China from SHRIMP U-Pb zircon studies of granitoids. *Ore Geol. Rev.* 13, 275–291. doi:10.1016/s0169-1368(97)00022-x
- Wang, T., Guo, L., Zheng, Y., Donskaya, T., Gladkochub, D., Zeng, L., et al. (2012). Timing and processes of late mesozoic mid-lower-crustal extension in continental NE Asia and implications for the tectonic setting of the destruction of the north China craton: mainly constrained by zircon U-Pb ages from metamorphic core complexes. *Lithos* 154, 315–345. doi:10.1016/j.lithos.2012.07.020
- Wang, W., Yang, E. X., Zhai, M. G., Wang, S. J., Santosh, M., Du, L. L., et al. (2013). Geochemistry of 2.7 Ga basalts from taishan area: Constraints on the evolution of early neoproterozoic granite-greenstone belt in Western Shandong province, China. *Precambrian Res.* 224, 94–109. doi:10.1016/j.precamres.2012.09.009
- Wang, J., Chang, S. C., Lin, P. J., Zhu, X. Q., Fu, Y. T., and Zhang, H. C. (2016). Evidence of Early Cretaceous transpression in the Sulu orogenic belt, eastern China. *Tectonophysics* 687, 44–55. doi:10.1016/j.tecto.2016.09.005
- Wang, C. C., Liu, Y. C., Zhang, P. G., Zhao, G. C., Wang, A. D., and Song, B. (2017). Zircon U-Pb geochronology and geochemistry of two types of Paleoproterozoic granitoids from the southeastern margin of the North China Craton: Constraints on petrogenesis and tectonic significance. *Precambrian Res.* 303, 268–290. doi:10.1016/j.precamres.2017.04.015
- Wang, S. J., Wang, L., Ding, Y., and Wang, Z. C. (2020). Origin and tectonic implications of post-orogenic lamprophyres in the Sulu belt of China. *J. Earth Sci.* 31 (6), 1200–1215. doi:10.1007/s12583-020-1070-y
- Wu, Z. P., Hou, X., and Li, W. (2007). Discussion on Mesozoic basin patterns and evolution in the eastern North China block. *Geotect. Metallogenia* 31, 385–399. (in Chinese with English abstract). doi:10.16539/j.ddgzycxk.2007.04.001
- Wu, M. L., Zhao, G. C., Sun, M., Li, S. Z., Bao, Z. S., Tam, P. K., et al. (2014). Zircon U-Pb geochronology and Hf isotopes of major Lithologies from the Jiaodong terrane: Implications for the crustal evolution of the eastern block of the north China craton. *Lithos* 190–191, 71–84. doi:10.1016/j.lithos.2013.12.004
- Wu, C., Liu, C. F., Zhu, Y., Zhou, Z. G., Jiang, T., Liu, W. C., et al. (2016). Early paleozoic magmatic history of central inner Mongolia, China: implications for the tectonic evolution of the southeast central asian orogenic belt. *Int. J. Earth Sci.* 105 (5), 1307–1327. doi:10.1007/s00531-015-1250-7
- Xia, Z. M., Liu, J. L., Ni, J. L., Zhang, T. T., Shi, X. M., and Wu, Y. (2016). Structure, evolution and regional tectonic implications of the Queshan metamorphic core complex in eastern Jiaodong Peninsula of China. *Sci. China Earth Sci.* 59 (5), 997–1013. doi:10.1007/s11430-015-5259-3

- Xie, S. W., Wu, Y. B., Zhang, Z. M., Qin, Y. C., Liu, X. C., Wang, H., et al. (2012). U–Pb ages and trace elements of detrital zircons from early cretaceous sedimentary rocks in the Jiaolai basin, north margin of the Sulu UHP terrane: provenances and tectonic implications. *Lithos* 154, 346–360. doi:10.1016/j.lithos.2012.08.002
- Xie, S. W., Xie, H. Q., Wang, S. J., Kröner, A., Liu, S. J., Zhou, H. Y., et al. (2014). Ca. 2.9 Ga granitoid magmatism in eastern Shandong, north China craton: Zircon dating, Hf–in–zircon isotopic analysis and whole-rock geochemistry. *Precambrian Res.* 255, 538–562. doi:10.1016/j.precamres.2014.09.006
- Xie, S. W., Wang, F., and Liu, Q. (2022). Petrogenesis and tectonic significance of mid-Paleoproterozoic granitic gneisses in the Jiaobei terrane, North China Craton: Constraints from SHRIMP zircon U–Pb dating and whole-rock geochemistry. *Acta Pet. Mineral.* 41 (2), 371–395. (in Chinese with English abstract).
- Xu, J. Q., and Li, Z. (2015). Middle–late mesozoic sedimentary provenances of the Luxi and Jiaolai areas: Implications for tectonic evolution of the north China block. *J. Asian Earth Sci.* 111, 284–301. doi:10.1016/j.jseas.2015.07.008
- Xu, Y. G., Huang, X. L., Ma, J. L., Wang, Y. B., Iizuka, Y., Xu, J. F., et al. (2004). Crust–mantle interaction during the tectono–thermal reactivation of the north China craton: Constraints from SHRIMP zircon U–Pb chronology and geochemistry of mesozoic plutons from Western Shandong. *Contrib. Mineral. Pet.* 147, 750–767. doi:10.1007/s00410-004-0594-y
- Xu, W. L., Hergt, J. M., Gao, S., Pei, F. P., Wang, W., and Yang, D. B. (2008). Interaction of adakitic melt–peridotite: implications for the high–Mg# signature of mesozoic adakitic rocks in the Eastern North China craton. *Earth Planet. Sci. Lett.* 265, 123–137. doi:10.1016/j.epsl.2007.09.041
- Xu, Y. G., Li, H. Y., Pang, C. J., and He, B. (2009). On the timing and duration of the destruction of the North China Craton. *Sci. Bull. (Beijing)*. 54, 3379–3396. doi:10.1007/s11434-009-0346-5
- Xu, J. Q., Li, Z., and Shi, Y. H. (2013). Jurassic detrital zircon U–Pb and Hf isotopic geochronology of Luxi Uplift, eastern North China, and its provenance implications for tectonic–paleogeographic reconstruction. *J. Asian Earth Sci.* 78, 184–197. doi:10.1016/j.jseas.2013.05.024
- Xu, H. J., Zhang, J. F., Wang, Y. F., and Liu, W. L. (2016). Late triassic alkaline complex in the Sulu UHP terrane: implications for post–collisional magmatism and subsequent fractional crystallization. *Gondwana Res.* 35, 390–410. doi:10.1016/j.gr.2015.05.017
- Yang, J. S., Wooden, J. L., Wu, C. L., Liu, F. L., Xu, Z. Q., Shi, R. D., et al. (2003). SHRIMP U–Pb dating of coesite-bearing zircon from the ultrahigh–pressure metamorphic rocks, Sulu terrane, east China. *J. Metamorph. Geol.* 21, 551–560. doi:10.1046/j.1525-1314.2003.00463.x
- Yang, J. H., Chung, S. L., Wilde, S. A., Wu, F. Y., Chu, M. F., Lo, C. H., et al. (2005a). Petrogenesis of post–orogenic syenites in the Sulu orogenic belt, east China: Geochronological, geochemical and Nd–Sr isotopic evidence. *Chem. Geol.* 214, 99–125. doi:10.1016/j.chemgeo.2004.08.053
- Yang, J. H., Wu, F. Y., Chung, S. L., Wilde, S. A., Chu, M. F., Lo, C. H., et al. (2005b). Petrogenesis of Early Cretaceous intrusions in the Sulu ultrahigh–pressure orogenic belt, east China and their relationship to lithospheric thinning. *Chem. Geol.* 222 (3), 200–231. doi:10.1016/j.chemgeo.2005.07.006
- Yang, J. H., Wu, F. Y., Shao, J. A., Wilde, S. A., Xie, L. W., and Liu, X. M. (2006). Constraints on the timing of uplift of the Yanshan Fold and Thrust belt, north China. *Earth Planet. Sci. Lett.* 246, 336–352. doi:10.1016/j.epsl.2006.04.029
- Yang, J. S., Li, T. F., Chen, S. Z., Wu, C. L., Robinson, P. T., Liu, D. Y., et al. (2009). Genesis of garnet peridotites in the Sulu UHP belt: Examples from the Chinese continental scientific drilling project–main hole, PP1 and PP3 drill holes. *Tectonophysics* 475, 359–382. doi:10.1016/j.tecto.2009.02.032
- Yang, D. B., Xu, W. L., Pei, F. P., Yang, C. H., and Wang, Q. H. (2012). Spatial extent of the influence of the deeply subducted South China block on the southeastern North China block: Constraints from Sr–Nd–Pb isotopes in mesozoic mafic igneous rocks. *Lithos* 136–139, 246–260. doi:10.1016/j.lithos.2011.06.004
- Yang, D. B., Xu, W. L., Xu, Y. G., Pei, F. P., and Wang, F. (2013). Provenance of sediments from mesozoic basins in Western Shandong: Implications for the evolution of the Eastern North China block. *J. Asian Earth Sci.* 76, 12–29. doi:10.1016/j.jseas.2013.07.027
- Yang, J. H., Xu, L., Sun, J. F., Zeng, Q., Zhao, Y. N., Wang, H., et al. (2021). Geodynamics of decratonization and related magmatism and mineralization in the North China Craton. *Sci. China Earth Sci.* 64 (9), 1409–1427. doi:10.1007/s11430-020-9732-6
- Yang, J. S., Liu, F. L., Wu, C. L., Xu, Z. Q., Shi, R. D., Chen, S. Y., et al. (2005c). Two ultrahigh–pressure metamorphic events recognized in the central orogenic belt of China: Evidence from the U–Pb dating of coesite-bearing zircons. *Int. Geol. Rev.* 47, 327–343. doi:10.2747/0020-6814.47.4.327
- Zhai, M. G., Zhao, L., Zhu, X. Y., Zhou, Y. Y., Peng, P., Guo, J. H., et al. (2021). Late Neoproterozoic magmatic–metamorphic event and crustal stabilization in the north China Craton. *Am. J. Sci.* 321, 206–234. doi:10.2475/01.2021.06
- Zhai, M. G. (2004). “Precambrian tectonic evolution of the north China craton,” in *Aspects of the tectonic evolution of China*. Editors J. Malpas, C. J. N. Fletcher, J. R. Ali, and J. C. Aitchison (Geological Society, London, Special Publications), 226, 57–72.
- Zhang, H. F., Gao, S., Zhong, Z. Q., Zhang, B. R., Zhang, L., and Hu, S. (2002a). Geochemical and Sr–Nd–Pb isotopic compositions of cretaceous granitoids: Constraints on tectonic framework and crustal structure of the dabieshan ultrahigh–pressure metamorphic belt, China. *Chem. Geol.* 186, 281–299. doi:10.1016/s0009-2541(02)00006-2
- Zhang, H. F., Sun, M., Zhou, X. H., Fan, W. M., Zhai, M. G., and Ying, J. F. (2002b). Mesozoic lithosphere destruction beneath the north China craton: Evidence from major trace element and Sr–Nd–Pb isotope studies of Fangcheng basalts. *Contrib. Mineral. Pet.* 23 (2), 241–254. doi:10.1007/s00410-002-0395-0
- Zhang, S. H., Zhao, Y., Song, B., and Yang, Y. H. (2007a). Zircon SHRIMP U–Pb and *in-situ* Lu–Hf isotope analyses of a tuff from western Beijing: Evidence for missing late Paleozoic arc volcano eruptions at the northern margin of the north China block. *Gondwana Res.* 12, 157–165. doi:10.1016/j.gr.2006.08.001
- Zhang, S. H., Zhao, Y., Song, B., and Liu, D. Y. (2007b). Petrogenesis of the Middle Devonian Gushan diorite pluton on the northern margin of the North China block and its tectonic implications. *Geol. Mag.* 144, 553–568. doi:10.1017/s0016756807003275
- Zhang, S. H., Zhao, Y., Liu, X. C., Liu, D. Y., Chen, F. K., Xie, L. W., et al. (2009a). Late paleozoic to early mesozoic mafic–ultramafic complexes from the northern North China block: Constraints on the composition and evolution of the lithospheric mantle. *Lithos* 110, 229–246. doi:10.1016/j.lithos.2009.01.008
- Zhang, S. H., Zhao, Y., Song, B., Hu, J. M., Liu, S. W., Yang, Y. H., et al. (2009b). Contrasting late carboniferous and late permian–middle triassic intrusive suites from the northern margin of the north China craton: Geochronology, petrogenesis, and tectonic implications. *Geol. Soc. Am. Bull.* 121 (1–2), 181–200. doi:10.1130/b261571
- Zhang, S. H., Zhao, Y., Kröner, A., Liu, X. M., Xie, L. W., and Chen, F. K. (2009c). Early permian plutons from the northern North China block: Constraints on continental arc evolution and convergent margin magmatism related to the central asian orogenic belt. *Int. J. Earth Sci.* 98 (6), 1441–1467. doi:10.1007/s00531-008-0368-2
- Zhang, J., Zhao, Z. F., Zheng, Y. F., and Dai, M. N. (2010). Postcollisional magmatism: Geochemical constraints on the petrogenesis of Mesozoic granitoids in the Sulu orogen, China. *Lithos* 119, 512–536. doi:10.1016/j.lithos.2010.08.005
- Zhang, H. F., Ying, J. F., Tang, Y. J., Li, X. H., Feng, C., and Santosh, M. (2011). Phanerozoic reactivation of the Archean North China craton through episodic magmatism: Evidence from zircon U–Pb geochronology and Hf isotopes from the Liaodong Peninsula. *Gondwana Res.* 19, 446–459. doi:10.1016/j.gr.2010.09.002
- Zhang, J., Zhao, Z. F., Zheng, Y. F., Liu, X. M., and Xie, L. W. (2012). Zircon Hf–O isotope and whole-rock geochemical constraints on origin of postcollisional mafic to felsic dykes in the Sulu orogen. *Lithos* 136–139, 225–245. doi:10.1016/j.lithos.2011.06.006
- Zhang, L. M., Wang, C. S., Cao, K., Wang, Q., Tan, J., and Gao, Y. (2016). High elevation of Jiaolai basin during the late cretaceous: Implication for the coastal mountains along the East asian margin. *Earth Planet. Sci. Lett.* 456, 112–123. doi:10.1016/j.epsl.2016.09.034
- Zhao, G. C., Sun, M., Wilde, S. A., and Li, S. Z. (2003). Assembly, accretion and breakup of the paleo–mesoproterozoic Columbia supercontinent: Records in the north China craton. *Gondwana Res.* 6, 417–434. doi:10.1016/s1342-937x(05)70996-5
- Zheng, J. P., Zhang, R. S., Yu, C. M., Tang, H. Y., and Zhang, P. (2004). *In-situ* zircon Hf isotopic, U–Pb age and trace element study of monzonite xenoliths from pingqun and Fuxin basalts: tracking the thermal events of 169 Ma and 107 Ma in Yanliao area. *Sci. China Ser. D.* 47, 39–52. doi:10.1360/04zd0023
- Zheng, Y. F., Zhao, Z. F., Wu, Y. B., Zhang, S. B., Liu, X., and Wu, F. Y. (2006). Zircon U–Pb age, Hf and O isotope constraints on protolith origin of ultrahigh–pressure eclogite and gneiss in the Dabie orogen. *Chem. Geol.* 231, 135–158. doi:10.1016/j.chemgeo.2006.01.005
- Zheng, Y. F., Gong, B., Zhao, Z. F., Wu, Y. B., and Chen, F. K. (2008). Zircon U–Pb age and O isotope evidence for Neoproterozoic low–¹⁸O magmatism during supercontinental rifting in South China: Implications for the snowball Earth event. *Am. J. Sci.* 308, 484–516. doi:10.2475/04.2008.04
- Zhou, J. B., Wilde, S., Zhao, G. C., Zhang, X. Z., Zheng, C. Q., Jin, W., et al. (2008). SHRIMP U–Pb zircon dating of the wulian complex: defining the boundary between the north and South China cratons in the Sulu orogenic belt, China. *Precambrian Res.* 162, 559–576. doi:10.1016/j.precamres.2007.10.008
- Zhu, R. X., Yang, J. H., and Wu, F. Y. (2012). Timing of destruction of the north China craton. *Lithos* 149 (4), 51–60. doi:10.1016/j.lithos.2012.05.013
- Zong, K. Q., Klemd, R., Yuan, Y., He, Z. Y., Guo, J. L., Shi, X. L., et al. (2017). The assembly of Rodinia: The correlation of early Neoproterozoic (ca. 900 Ma) high–grade metamorphism and continental arc formation in the southern Beishan Orogen, southern Central Asian Orogenic Belt (CAOB). *Precambrian Res.* 290, 32–48. doi:10.1016/j.precamres.2016.12.010